*International Geology Review*, 2014
Vol. 56, No. 15, 1813–1836, http://dx.doi.org/10.1080/00206814.2014.954279

Taylor & Francis
Taylor & Francis Group

# Late Cretaceous extension and Palaeogene rotation-related contraction in Central Anatolia recorded in the Ayhan-Büyükkışla basin

Eldert L. Advokaat[a,b], Douwe J.J. van Hinsbergen[a]*, Nuretdin Kaymakcı[c,d], Reinoud L.M. Vissers[a] and Bart W. H. Hendriks[e]

[a]*Department of Earth Sciences, University of Utrecht, Utrecht, The Netherlands;* [b]*SE Asia Research Group, Department of Earth Sciences, Royal Holloway University of London, Egham, UK;* [c]*Middle East Technical University, Department of Geological Engineering, Ankara, Turkey;* [d]*Palaeomagnetic Laboratory 'Fort Hoofddijk', Department of Earth Sciences, University of Utrecht, Utrecht, The Netherlands;* [e]*Centre for Geodynamics, Geological Survey of Norway (NGU), Trondheim, Norway*

(*Received 10 March 2014; accepted 10 August 2014*)

The configuration and evolution of subduction zones in the Eastern Mediterranean region in Cretaceous time accommodating Africa–Europe convergence remain poorly quantitatively reconstructed, owing to a lack of kinematic constraints. A recent palaeomagnetic study suggested that the triangular Central Anatolian Crystalline Complex (CACC) consists of three blocks that once formed an ~N–S elongated continental body, underthrusted below ophiolites in Late Cretaceous time. After extensional exhumation and upon Palaeogene collision of the CACC with the Pontides of the southern Eurasian margin, the CACC broke into three fragments that rotated and converged relative to each other. Here, we date the extension and contraction history of the boundary between two of the rotating massifs of the CACC by studying the Upper Cretaceous–Palaeogene Ayhan–Büyükkışla basin. We report an $^{40}Ar/^{39}Ar$ age of an andesite at the base of the sequence to show that the deposition started in an E–W extensional basin around 72.11 ± 1.46. The basin developed contemporaneously with regional exhumation of the CACC metamorphics. The lower basin sedimentary rocks were unconformably covered by mid-Eocene limestones and redbeds, followed by intense folding and thrust faulting. Two balanced cross-sections in the study area yield a minimum of 17–27 km of post-mid-Eocene ~N–S shortening. We thus demonstrate the Cenozoic compressional nature of the Kırşehir–Niğde-Hırkadağ block boundary and show that the extensional exhumation of the CACC predates collision-related contraction. A plate kinematic scenario is required to explain these observations that involves two Late Cretaceous–Palaeogene subduction zones to the north and south of the CACC, for which we show a possible plate boundary configuration.

**Keywords:** Turkey; geodynamics; tectonics; basin; Ar/Ar dating



## 1. Introduction

Closure of the Neotethyan oceanic domain was associated with the subduction of oceanic and continental lithosphere below continental and oceanic plates and led to Jurassic and younger deformation, magmatism, and metamorphism in the eastern Mediterranean region (Sengör and Yilmaz 1981; Dercourt *et al.* 1986; Stampfli and Hochard 2009). In the Aegean region, Late Cretaceous and younger Africa–Europe convergence was accommodated along a single subduction zone below the Eurasian continental margin and was associated with accretion of continental and oceanic (upper) crust to the overriding plate, forming an elevated fold–thrust belt (Faccenna *et al.* 2003; van Hinsbergen *et al.* 2005, 2010; Jolivet and Brun 2010). Subsequently, during periods of slab rollback, the previously buried and metamorphosed parts of the fold–thrust belt became exhumed as a result of widespread extension of the overriding plate (Dilek and Altunkaynak 2007, 2009; Dilek and Sandvol 2009; Edwards and Grasemann 2009; Jolivet *et al.* 2009; Jolivet and Brun 2010; van Hinsbergen and Schmid 2012). In Anatolia, however, the tectonic accommodation of Africa–Europe convergence was more complex and was accommodated by multiple, partly synchronous subduction zones; many different scenarios for the number and configurations of subduction systems have been proposed (e.g. Stampfli and Borel 2002; Robertson 2004; Okay *et al.* 2006; Barrier and Vrielynck 2008; Moix *et al.* 2008; Lefebvre *et al.* 2013; Okay *et al.* 2013): the kinematic reconstruction of subduction systems in the eastern Mediterranean region proves to be challenging.

The Central Anatolian Crystalline Complex (CACC) in Turkey (Göncüoğlu *et al.* 1991) (Figure 1; also known as the Kırşehir Block (Görür *et al.* 1984)) is a key region in our attempts to reconstruct the eastern Mediterranean subduction zone configuration since the Late Cretaceous. The CACC is a 200 km × 200 km × 200 km, triangular continental domain surrounded by suture zone(s) and belts of high-pressure (HP) metamorphic rocks that demarcate former subduction zones.

To the north, the CACC is separated from the continental Pontides of the southern Eurasian margin by the Izmir–Ankara–Erzincan suture zone (IAESZ) (Sengör and

*Corresponding author. Email: d.j.j.vanhinsbergen@uu.nl

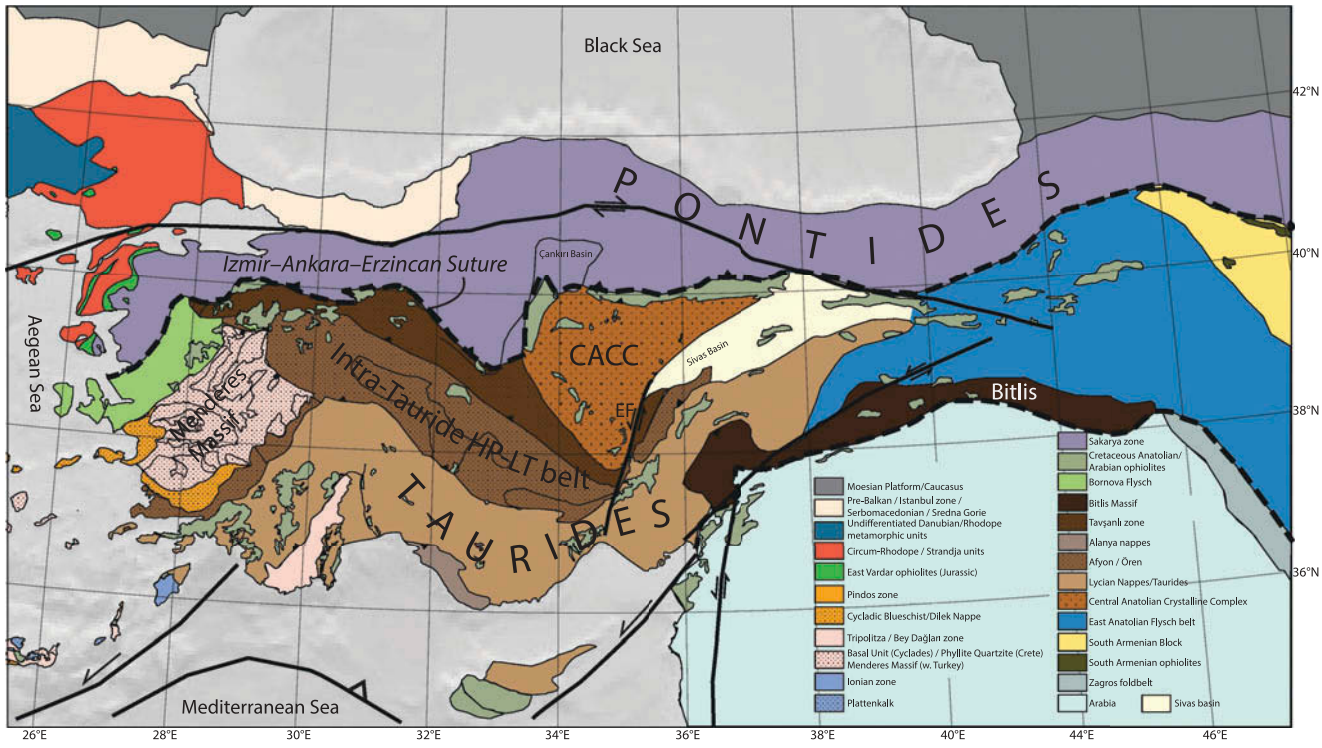


Figure 1. Tectonic map of the eastern Mediterranean region, modified after Okay *et al.* (1996), Şengör *et al.* (2008), Pourteau *et al.* (2010), and van Hinsbergen and Schmid (2012). EF = Ecemiş Fault.

Yilmaz 1981). Along the IAESZ, a northern branch of the Neotethyan Ocean subducted since at least the Early Cretaceous, as shown by HP metamorphic rocks, arc magmatism and deformation in the Pontides, and the evolution of a forearc basin along its southern margin (Tüysüz *et al.* 1995; Okay *et al.* 2001, 2006; Rice *et al.* 2006; Kaymakcı *et al.* 2009; Hippolyte *et al.* 2010; Okay *et al.* 2013). The CACC and overriding ophiolites started to collide with the Pontides in latest Cretaceous to Palaeocene time, shown by a transition from forearc to foreland basin evolution along the southern Pontide margin and formation of a northward convex orocline in the Pontides north of the CACC (Görür *et al.* 1984, 1998; Kaymakci *et al.* 2003, 2009; Meijers *et al.* 2010) (Figure 1).

Fringing the CACC to the south are belts of high-pressure, low-temperature (HP-LT) metasedimentary rocks, known as the older, structurally higher, and higher pressure Tavsanli and the younger, structurally lower, and lower pressure Afyon zones (Okay *et al.* 1996; Okay and Tüysüz 1999; Dilek and Whitney 1997; Pourteau *et al.* 2010, 2013; Whitney *et al.* 2011). Based on $^{40}Ar/^{39}Ar$ mica ages, and unconformably overlying sedimentary rocks of these belts in western Turkey, a ca. 88–55 Ma history of burial and exhumation was inferred for these belts, with these processes younging towards deeper structural levels (Sherlock *et al.* 1999; Seaton *et al.* 2009; Pourteau *et al.* 2013). These data have been interpreted to infer a second Late Cretaceous subduction zone to the south of the CACC, commonly referred to as the 'Intra-Tauride' subduction zone (Sengör and Yilmaz 1981; Dilek and Whitney 1997; Dilek *et al.* 1999; Parlak and Robertson 2004; Clark and Robertson 2005; Barrier and Vrielynck 2008; Robertson *et al.* 2009; Sarıfakıoğlu *et al.* 2013).

The CACC itself exposes metasedimentary rocks that underwent regional Barrovian metamorphism following ophiolite obduction of Late Cretaceous age (Santonian–Turonian, ca. 90–85 Ma) (Erkan 1976; Seymen 1981; Göncüoğlu 1986; Erdogan *et al.* 1996; Yalınız and Göncüoğlu 1998). After ophiolite emplacement and regional metamorphism followed the intrusion of an Upper Cretaceous belt of plutons geochemically consistent with arc magmatism (Göncüoğlu 1986; Kadioglu *et al.* 2003, 2006; Köksal *et al.* 2004; Ilbeyli 2005; Boztuğ *et al.* 2007, 2009a). Exhumation of the CACC metamorphics is documented by geochronology and low-temperature thermochronology to occur ca. 75–60 Ma and was in several places shown to have been accommodated by low-angle extensional shear zones and detachment faults (Göncüoğlu 1986; Whitney *et al.* 2003; Köksal *et al.* 2004; Whitney and Hamilton 2004; Boztuğ and Jonckheere 2007; Boztuğ *et al.* 2007, 2009b; Gautier *et al.* 2008; Isik *et al.* 2008; Isik 2009; Lefebvre 2011; Lefebvre *et al.* 2011).

To unravel the plate tectonic configuration and geodynamic evolution of the Cretaceous–Palaeogene subduction–collision history of Anatolia, it is essential to

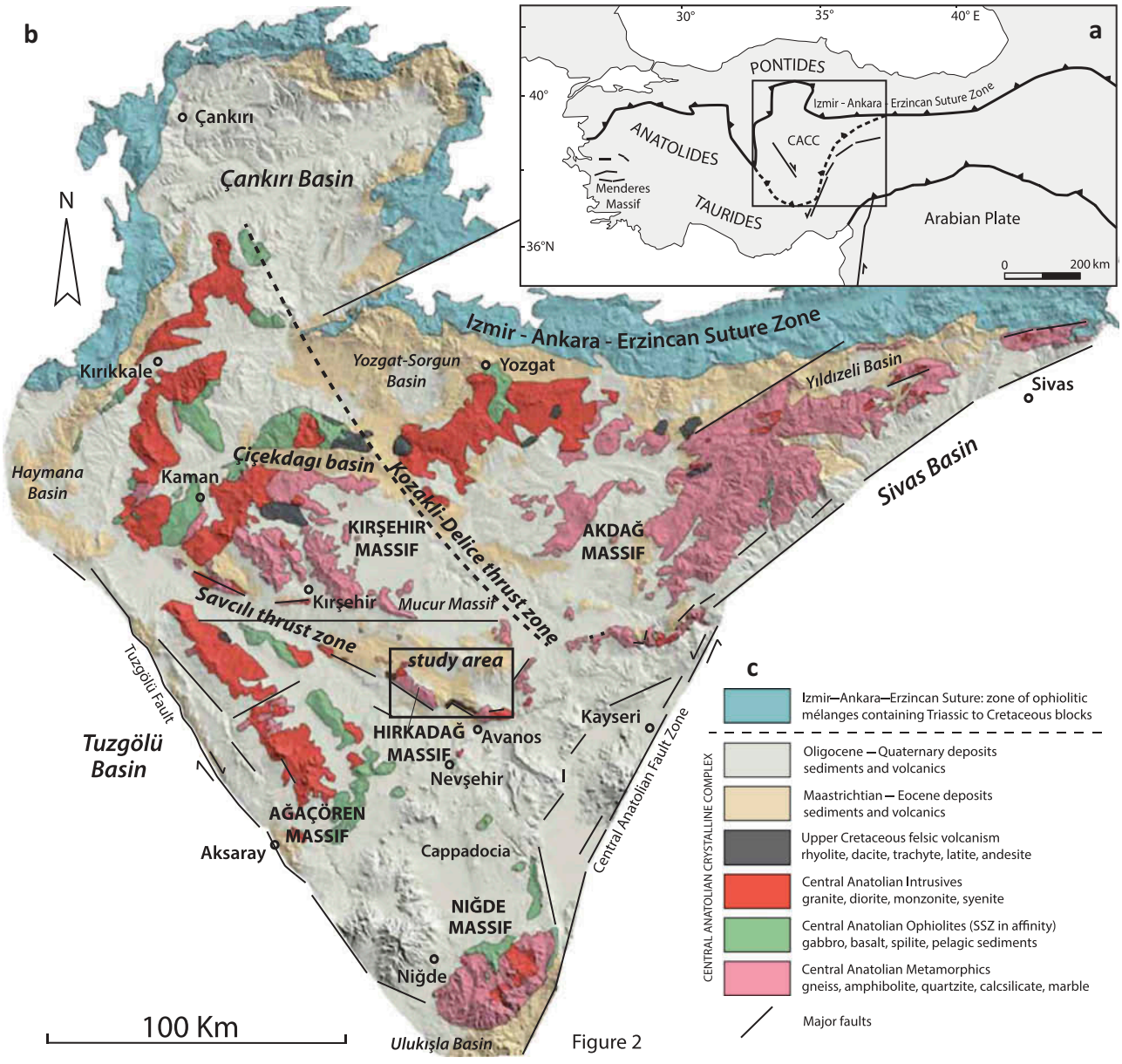


Figure 2. (a) Location of the Menderes Massif and the CACC in the Turkish orogenic system. (b) Simplified geological map of the CACC projected on a digital elevation model. The black rectangle indicates the area of study presented in Figure 2. (c) Simplified tectonostratigraphic column showing the relationships between the main units of the CACC (not to scale). SSZ, supra-subduction zone.

develop accurate kinematic reconstructions and, in particular, to restore the Late Cretaceous configuration of the CACC preceding its collision with the Pontides. Towards this end, Lefebvre *et al.* (2013) recently carried out a palaeomagnetic study of the granitoid belts in the CACC. Their results demonstrated that the massif contains three internally palaeomagnetically coherent blocks (the Akdağ, Kırşehir, and Niğde-Ağaçören massifs, Figure 2) that rotated relative to each other after latest Cretaceous cooling of the granitoids (Figure 3). Correcting for these rotations aligns the granitoid belts into a Late Cretaceous ~N–S trend and suggests that documented extensional shear zones and detachment faults accommodated ~E–W extension. This configuration is somewhat surprising, since Africa–Europe convergence in Late Cretaceous times occurred in a NNE–SSW direction (Torsvik *et al.* 2012): it would suggest that a highly oblique, N–S striking subduction zone may have existed that created E–W overriding plate extension.

Lefebvre *et al.* (2013) proposed that the Central Anatolian block rotations were accommodated along two fault zones (Figure 3). One of these is the Savcılı thrust zone (Görür *et al.* 1998; Yürür and Genç 2006; Isik *et al.* 2014), which should accommodate several tens of

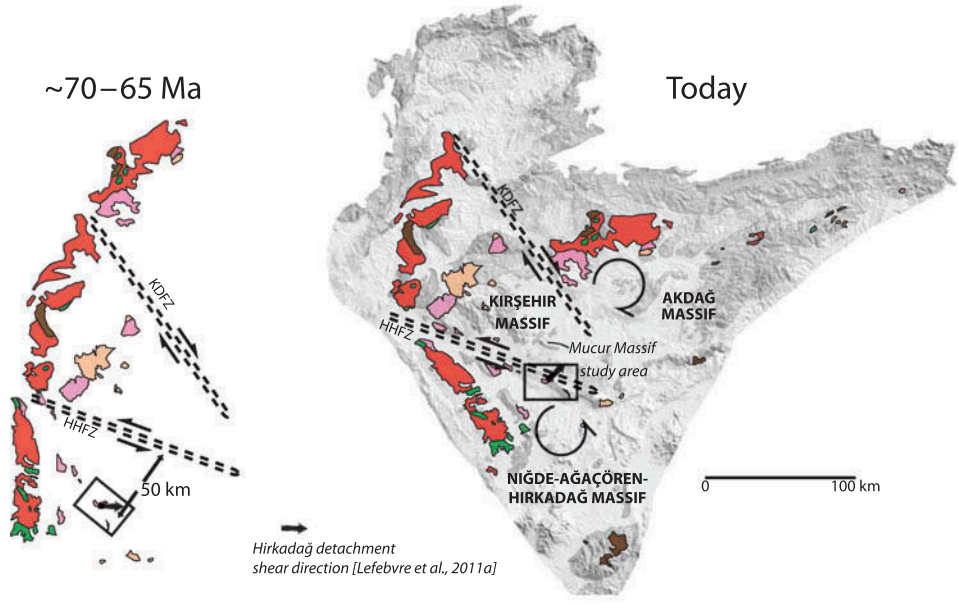


Figure 3. Present-day (right-hand side) and Late Cretaceous (left-hand side) configuration of the magmatic belts of the CACC according to palaeomagnetic results, modified from Lefebvre *et al.* (2013). The fault zone parallel to the Savcılı thrust zone was proposed by these authors as a transpressional fault zone that accommodated a 29.0 ± 4.5° counterclockwise rotation of the Niğde–Ağaçören massif in the south relative to the Kırşehir Massif in the north, which would require ~40–60 km of total N(NE)–S(SW) shortening. If correct, this would restore the sense of shear recorded along the Hırkadağ detachment (Lefebvre 2011) into a top-to-the-E Late Cretaceous orientation.

kilometres shortening to accommodate the palaeomagnetically determined ~30° rotation between the Kırşehir and Niğde–Ağaçören massifs (Lefebvre *et al.* 2013) (Figures 2 and 3). In this article, we test that prediction by studying the structural and stratigraphic evolution of the Ayhan–Büyükkışla basin that lies within the postulated Savcılı thrust zone (Figures 2 and 3) and aim to obtain constraints on the timing of central Anatolian rotational deformation.

The Ayhan–Büyükkışla basin is located adjacent to the Hırkadağ massif, along the northern edge of the counterclockwise rotated Niğde–Ağaçören massif. The basin exposes a folded and thrust faulted stratigraphy of volcanic, continental clastic, and shallow marine and lacustrine calcareous rocks, with a presumed Late Cretaceous to post-mid Eocene age range (Göncüoğlu *et al.* 1993; Köksal and Göncüoğlu 1997; Köksal *et al.* 2001). Here, we report the results from mapping of the stratigraphy and structure of the Ayhan–Büyükkışla basin, geochronological dating of its volcanic content, and cross-section restoration of its compressional history. We evaluate our results within the context of the Late Cretaceous–Palaeogene kinematic evolution of Central Anatolia and the subduction zone configuration inferred from that.

## 2. Geological setting

The oldest and tectonostratigraphically deepest rocks in the CACC comprise metasedimentary rocks with presumably Palaeozoic to Lower Cretaceous sedimentary protoliths (Göncüoğlu *et al.* 1992; Kocak and Leake 1994). These are tectonically overlain by the Central Anatolian Ophiolites, with Turonian–Santonian crustal ages (Seymen 1981; Yalınız and Göncüoğlu 1998; Floyd *et al.* 2000; Yalınız *et al.* 2000; Lefebvre *et al.* 2011), intruded by a regionally extensive suite of granitoids, with local gabbros and syenitoids (Figure 2) with published ages covering the ca. 95–75 Ma interval (Göncüoğlu 1986; Kadioglu *et al.* 2003; Whitney *et al.* 2003; Köksal *et al.* 2004; Boztuğ *et al.* 2007, 2009a; Lefebvre 2011). An 84.1 ± 0.8 Ma U/Pb monazite age from migmatites in the Kırşehir Massif was interpreted to date peak metamorphic conditions in the CACC (Whitney and Hamilton 2004). Because the granitoid suites did not experience the intense prograde to syn-peak metamorphic deformation characteristic of the CACC metamorphics, the pre-85 Ma magmatic ages may be incorrect (Lefebvre *et al.* 2013).

The tectonic causes of exhumation of the high-grade metamorphic rocks of the CACC remain only locally resolved, but are consistent with a key role of extensional denudation (Whitney and Dilek 1997; Gautier *et al.* 2002, 2008; Isik *et al.* 2008; Isik 2009; Lefebvre 2011; Lefebvre *et al.* 2011). Following initial postulations that extensional exhumation occurred in the Miocene (Whitney and Dilek 1997), subsequent evidence has demonstrated that the timing of extensional exhumation is mainly Late Cretaceous to perhaps Palaeocene in age (~75–60 Ma)

(Boztuğ and Jonckheere 2007; Gautier *et al.* 2008; Isik *et al.* 2008; Boztuğ *et al.* 2009a; 2009b; Isik 2009; Lefebvre *et al.* 2011). Extension-related deformation was overprinted by contractional deformation that developed in the localized zones of folding and thrust faulting, such as the Savcılı thrust zone, of which recent clay mineral dating in gouges suggested that it has been active between 46–40 and 29–22 Ma (Isik *et al.* 2014), and the Çiçekdağı syncline and Çiçekdağı basin that formed between 39 and 35 Ma (Gülyüz *et al.* 2013) (Figure 2).

To the southwest and southeast of the Ayhan–Büyükkışla basin, the study area of this article (Figure 4), metamorphic and plutonic rocks are exposed in the Hırkadağ massif and in the İdiş Dağı block, respectively, exposing amphibolite-facies metasedimentary rocks, intruded by granodiorites and syenites (Whitney and Dilek 2001; Lefebvre 2011). In the southeast of the study area, near Göynük village, a thrust fault emplaces syenites of the İdiş Dağı block over continental clastic sedimentary rocks that intercalate with mafic volcanics that were correlated to regionally occurring (Karahıdır) volcanics of a Late Cretaceous age (Aydın 1985; Gökten and Floyd 1987; Kara and Dönmez 1990; Göncüoğlu *et al.* 1993) (Figure 4). These mafic volcanics are probably magmatically cogenetic and consequently contemporaneous with the İdiş Dağı syenite (Köksal *et al.* 2001). Clastic sedimentary rocks and volcanics with a presumed Late Cretaceous age are also exposed in the central part of our study area around Ayhan between the İdiş Dağı and Hırkadağ blocks (Atabey 1989) (Figure 4). Overlying the continental clastic series in the Ayhan area are Eocene nummulitic limestones, dated as Lutetian (48.6–40.4 Ma in the timescale of (Gradstein *et al.* 2004)) based on their alveolina and nummulite content (Göncüoğlu *et al.* 1993), overlain by unfossiliferous (probably lacustrine) marls. Eocene limestones are widespread in central Anatolia and frequently unconformably cover exhumed metamorphic basement of the CACC (e.g. Göncüoğlu *et al.* 1991; Gülyüz *et al.* 2013).

The Eocene and older units in the Ayhan area are unconformably overlain by a series of folded and thrust faulted red fluvial conglomerates, covering the northern

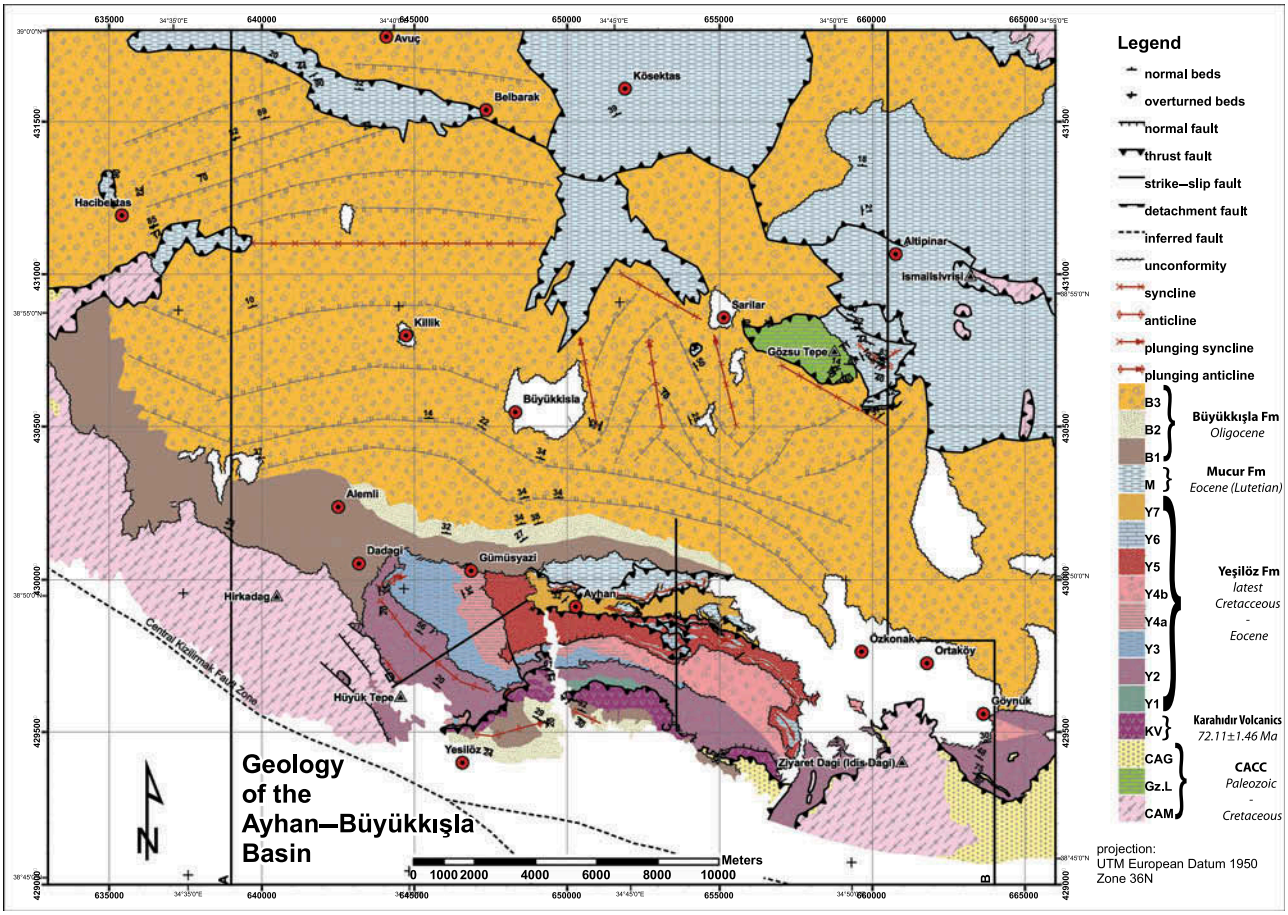


Figure 4. Geological map of the Ayhan–Büyükkışla basin. The stratigraphic units that we mapped are outlined in Figure 5. For profiles A and B, see Figure 9. CAG, Central Anatolian Granites; CAM, Central Anatolian Metamorphics; GzL, Gözsu Tepe Limestone; KV, Karahıdır volcanics.

half of the study area around Büyükkışla (Figure 4). The age of the Büyükkışla basin fill is Lutetian or younger, as it covers the limestones, and is generally assumed to be Oligocene (Atabey 1989), but no independent age data exist. In the north of the study area (Figure 4), Eocene limestones and marls are exposed, and the northern contact between the Büyükkışla redbeds and Eocene limestones was previously mapped as an unconformity (Atabey 1989). The study area is bounded in the south by a normal fault that has Miocene (Tortonian) and younger volcanic tuff, commonly referred to as the Ürgüp Formation of the Cappadocian volcanic province, in its hanging wall (Atabey 1989; Mues-Schumacher and Schumacher 1996; Viereck-Goette *et al.* 2010). In places, subhorizontal tuffs unconformably cover all previous units in the study area.

## 3. Lithostratigraphy of the Ayhan–Büyükkışla Basin

The oldest part of the stratigraphy – termed the Yeşilöz Formation and intercalating 'Karahıdır' volcanics – is exposed in the Ayhan and Göynük area (Figure 4). The overlying nummulitic limestones and marls are assigned to the Mucur Formation. The unconformably overlying series of ~5 km of red conglomerates and sandstones define the Büyükkışla Formation.

### 3.1. Yeşilöz Formation

The Ayhan area exposes an ~4 km-thick stratigraphy with internal low-angle unconformities. The volcanics intercalating at the base of the Yeşilöz Formation were previously assigned to the 'Göynük volcanoclastic olistostrome' (Köksal and Göncüoğlu 1997), described as containing continental clastic sedimentary rocks, blocks of volcanics as well as blocks of İdiş Dağı syenite. Our observations suggest, however, that such an amalgamation is restricted to a zone of ~50 m thickness below the İdiş Dağı thrust fault, and that this lithology represents a tectonic mélange related to post-depositional thrust faulting, not olistostromal processes. Immediately north of Göynük, a succession of intercalating purple and yellow lavas, stratified tuffs, conglomerates, and redbeds show that the volcanics form an integral part of the Yeşilöz Formation stratigraphy. In addition to the Karahıdır volcanics, we subdivide the Yeşilöz Formation into seven members that have been mapped separately to highlight the basin's structure (Y1–7) (Figure 5).

Member Y1 consists of alternating dark-grey mudstone without fossils and lens-shaped sandstones. It only crops out in the central southern part of the basin with an exposed thickness of 250 m, tapering out to the W. It was probably deposited in a fluvial environment.

The overlying Member Y2 consists of purple and red conglomerates and intercalated sandstones that can be

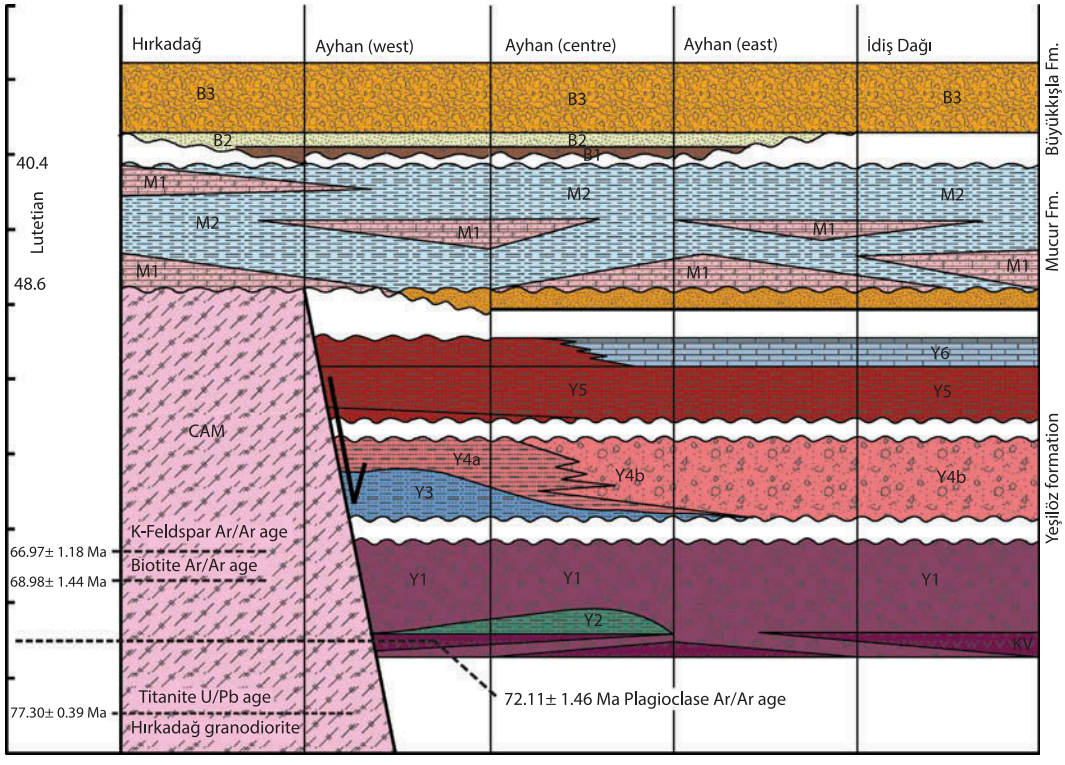


Figure 5. Facies diagram showing the regional and vertical relationships between the metamorphic basement of the Hırkadağ Block and the stratigraphy of the Ayhan–Büyükkışla basin.

traced all along the western and southern parts of the basin (Figure 4). Its thickness increases from ~600 m in the southeast to ~825 m in the southwest. The member consists of cross-bedded, fining upward sandstones, and up to 5 m-thick lenticular conglomerate beds that erode the underlying strata. The conglomerates are clast-supported, with sub-angular 10–50 cm clasts solely consisting of volcanic debris. Palaeocurrent directions in fluvial sandstones of this member are variable towards W and S (in present-day coordinates). The unit is interpreted as alternating braided fluvial and debris flow deposits constituting a continental clastic fan system. At the west bank of the Kızılöz river, andesite lavas intercalate with Member Y2, and we collected a sample (21-05) for $^{40}Ar/^{39}Ar$ geochronology (Figure 5).

Member Y3 overlies the underlying purple conglomerates, and the contact between these units in the west of the basin shows an ~15° angular unconformity. Member Y3 consists of ~1200 m of sandstones and blue-grey mudstones without fossils. The member tapers out to the E, where it is exposed in small lenses only, and may interfinger with Member Y4. Its lower 150 m consists of regular alternations of ~30 cm-thick, yellow, carbonate-rich, fine- to medium-grained sandstones intercalated with 2–4 m-thick siltstone and claystone layers. The upper ~1000 m consists of alternating blue mudstone and very fine-grained yellow sandstone. Slump structures are common (Figure 6). The basal sandstone preserves syn-sedimentary normal faults, suggesting a roughly E–W direction of extension in their present orientation (Figure 6). The palaeoenvironment is interpreted as fluvial for the basal sandstones and lacustrine for the upper 1000 m.

Member Y4 consists of an ~625 m-thick sequence of red sandstones. In the west, the base of the succession consists of medium- to coarse-grained, thick-bedded (1–2 m) grey sandstones. Upwards, fine- to medium-grained 5–15 cm-thick laminated sandstones occur that intercalate with 5–50 cm-thick red siltstones. In the east, the member consists of conglomerate, coarse sandstones, and siltstones. Conglomerates consist mainly of volcanic debris with ~5–10% granite and quartzite pebbles. The sequence is interpreted as deposited in a fluvial environment.

Member Y5 unconformably overlies Y4 with a low-angle unconformity and consists of 400 m of dark-red sandstones, thinning to 200 m eastwards. The sequence comprises one white-coloured sandstone of 20 m thickness, consisting of very coarse sandstones, followed by a poorly exposed sequence of fine laminated dark-red sandstones. The top of the formation is formed by intercalations of fine-bedded siltstone and claystone. The sequence is interpreted as a transition from a fluvial environment represented by the sandstones to a lacustrine environment represented by the siltstone and claystone.

Member Y6 is exposed in the eastern part of the basin and comprises ~100 m of 1–2 m-thick bedded limestones (mudstones), without macroscopically observable fossils. The sequence is interpreted as a lacustrine deposit laterally equivalent with the lacustrine rocks of Member Y5.

Finally, Member Y7 consists of 250 m of red sandstones and mudstone. The relationship with the underlying limestones is unknown, because the only contact with the limestones is a thrust fault. The sequence consists of 0.5–2 m-thick beds of coarse cross-bedded orange sandstones. The sequence is interpreted as fluvial.

### 3.2. *Mucur Formation*

The Mucur Formation overlies the Yeşilöz Formation with an ~5° angular unconformity and consists of two members (not specified as separate members on the map of Figure 4). Member 1 is exposed around Ayhan and comprises an ~200 m-thick sequence of 0.5–1 m thick, grain-supported beds of nummulites and alveolinae, and ~10 m-thick beds of pelecypoda and nummulites. These fossils clearly demonstrate a shallow marine environment. In Ayhan village, Göncüoğlu *et al.* (1993) assigned a Lutetian (48.6–40.4 Ma) age for these limestones. Member M1 is also found in the north and west of the study area, e.g. around Hacıbektaş and Avuç, where it is found in thrust fault contact above the Büyükkışla Formation. Around Avuç, the limestones are conformably overlain by Member M2, which consists of white to grey marls and mudstones with abundant organic matter fragments, alternating with sandstones and unfossiliferous limestones, generally of up to ~30 cm thick. The maximum observed thickness of Member M2 is ~300 m in the east of the study area. The member contains frequent large-scale (tens of metres in size) slumps. This sequence was previously suggested to be deep marine (Göncüoğlu *et al.* 1993), but the absence of marine fossils and the abundant presence of organic matter lead us to interpret a lacustrine palaeoenvironment instead.

### 3.3. *Büyükkışla Formation*

The Büyükkışla Formation is a monotonous, ~5 km-thick sequence of red siltstones with lenticular bodies of sandstone and conglomerate. The base of the stratigraphy directly north and south of the exposures of the Yeşilöz Formation contains two additional members with different colours, convenient for structural mapping. Hence, we subdivide the stratigraphy into three members (B1–3).

The lowermost Member B1 overlies the Mucur and Yeşilöz Formations and the Hırkadağ metamorphic basement with an angular unconformity. In the south, the contact between Member B1 and the Yeşilöz Formation is a normal fault, and northeast of Ayhan, the Yeşilöz and Mucur Formations are probably thrust faulted over the

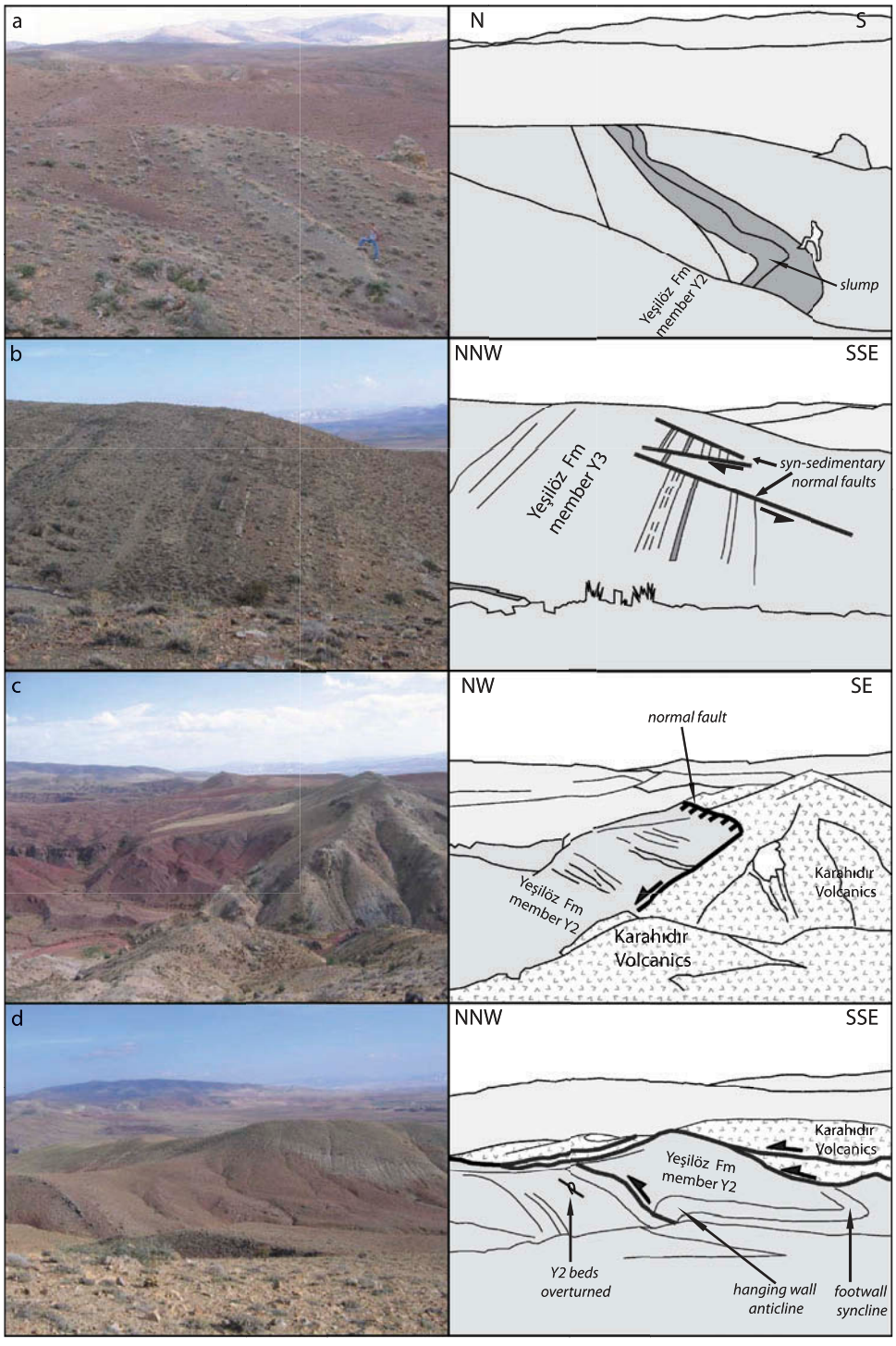


Figure 6. (a) Slump folding and (b) syn-sedimentary normal faulting in the Yeşilöz Formation. (c) Normal fault between the Karahıdır volcanics and the Yeşilöz Formation (Member Y2) in the southeast of the Ayhan area. Tapering features in Member Y2 show syn-sedimentary activity; (d) To the west, the normal fault is not visible, but instead, post-sedimentary thrust faults deform the Yeşilöz Formation.

Büyükkışla Formation (Figure 4). North of the Ayhan basin, Member B1 is ~450 m thick and consists of dark-red conglomerates and mudstones. The sequence contains a 150 m-thick conglomerate succession at the base made up of 5–30 cm sized pebbles of metamorphic rocks and granites. Pebble imbrication and cross-bedding indicate easterly directed palaeoflow (Figure 7). The basal conglomerates are followed by a 300 m-thick sequence of

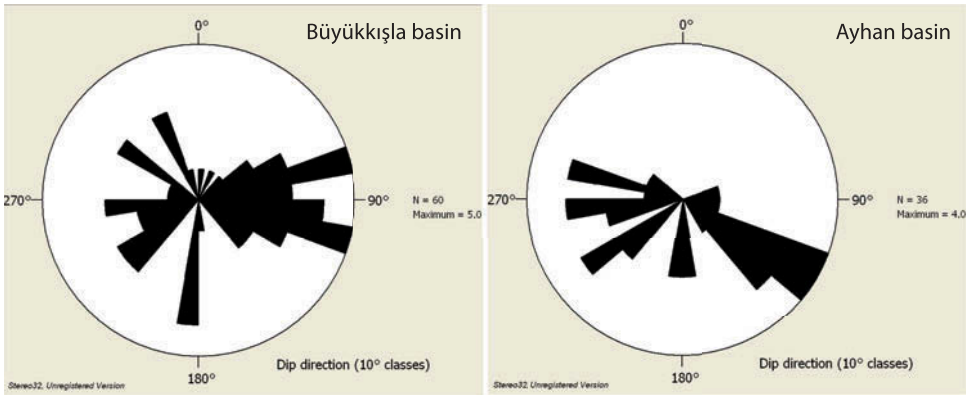


Figure 7. Palaeocurrent directions in the Ayhan–Büyükkışla basin, showing dominantly E–W- or W–E-trending palaeocurrents. For the Büyükkışla Formation, this is parallel to the fold axis of the Killik syncline. For the Yeşilöz Formation, this is parallel to the syn-sedimentary normal faults in the basin, with some palaeocurrent directions towards the southern N-dipping normal fault of Figure 6c.



5–20 cm-thick fine-grained sandstone beds intercalated with 5–50 cm-thick lignites, which are locally mined. We have been unable to derive pollen from these lignites for age dating. The sequence is interpreted as an alternation of braided fluvial and debris flow deposits. Upwards, the palaeoenvironment was dominated by fluvial deposits and marshes.

Member B2 consists of a 300 m-thick sequence of olive-green sandstones and mudstones, with a 100 m-thick sandstone at the base. It is succeeded by 200 m of alternating ~20 cm-thick fine-grained sandstone beds and 0.5–2 m-thick claystone layers. Lenticular sandstone bodies are erosive, 5–10 m thick, and 20–30 m wide. Cross-beds in the sandstone layers indicate westerly palaeoflow (Figure 7). Member B2 is interpreted to reflect a fluvial depositional environment, with channelled sandstone bodies and claystone-dominated overbank deposits.

Member B3 is not further subdivided and comprises the top ~4 km of the succession. It is dominated by orange fluvial sandstones, mudstones, and conglomerates, including matrix-supported conglomerate layers of up to 3 m thickness. These layers have moderately sorted, semi-rounded pebbles ranging in size from 4 to 10 cm. The pebble content is diverse and in the lower part of the sequence consists mainly of volcanics and some reworked sandstone, but higher in the sequence (near Sarılar) also fragments of nummulitic limestone were found. Sandstone layers are typically ~20 cm thick, with grain sizes between medium and very coarse sand. At the base of the succession, pebble imbrication and cross-beds indicate E-directed palaeoflow (Figure 7). The unit is interpreted as an alternating braided fluvial and debris flow deposit.

## 4. $^{40}Ar/^{39}Ar$ geochronology

Plagioclase was separated from sample 21-05 for $^{40}Ar/^{39}Ar$ geochronology. Figure 8 displays the spectrum and inverse isochron diagrams. Statistics on both the spectrum and the inverse isochron indicate some minor disturbance of the Ar isotope system. We define a plateau according to the following requirements: at least three consecutive steps, overlapping at the 95% confidence level, together comprising at least 50% of total $^{39}Ar$ and mean square of weighted deviates (MSWD) less than the two-tailed Student *T* (Stud-*T*) critical value. We use the weighted York-2 method to calculate the inverse isochron results, with statistically valid isochrons having a MSWD value less than the two-tailed *F*-test critical value. For sample 21-05, a weighted mean age of 72.06 ± 1.78 Ma ($2\sigma$) was determined (Figure 8) for 81.83% of the cumulative $^{39}Ar$. The ages and uncertainties for the three steps included in the calculation almost overlap at the $2\sigma$ level, but with a MSWD of 5.854 and a Stud-*T* value of 4.303 they do not constrain a true plateau. Steps 1–4, representing 91.61% of the cumulative $^{39}Ar$, yield a statistically valid (i.e. MSWD of 2.888 below the *F*-test value of 2.997) inverse isochron age of 72.11 ± 1.46 Ma ($2\sigma$). Again, some minor disturbance of the Ar isotope system is indicated by the $^{40}Ar/^{36}Ar$ ratio, which at 254.48 ± 22.87 ($2\sigma$) is lower than the atmospheric ratio. The weighted mean plateau age and the inverse isochron age nevertheless completely overlap.

## 5. Structure

### 5.1. *Present-day structure*

The angular unconformity between the Büyükkışla Formation and the underlying formations (Figure 4) suggests that the Yeşilöz and Mucur Formations have experienced at least one deformation phase more than the Büyükkışla Formation. Therefore, we first describe the deformation accommodated in the Büyükkışla Formation and then summarize the deformation in the area around Ayhan that exposes the older formations.

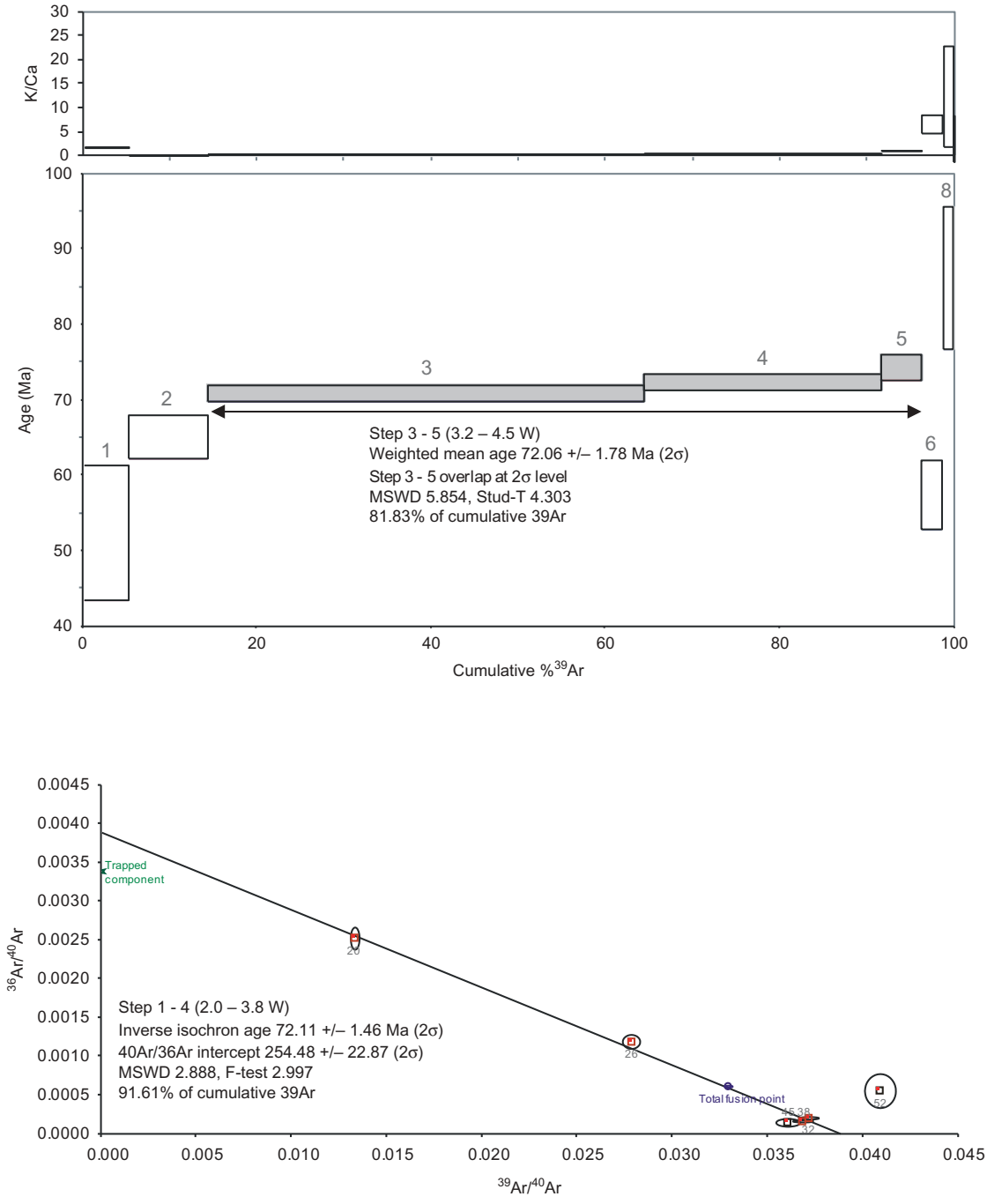


Figure 8. Step heating release spectra for sample 21-05 (plagioclase) from the Karahıdır volcanics. Each age bar is plotted at 95% confidence level. The numbers above the age bars correspond to the row number in the Appendix. The bottom panel shows the inverse isochron diagram, with numbers corresponding to the laser power in Watts.

A cross-section through the western part of the study area is shown in profile A of Figure 9. The Hırkadağ massif is bounded to the south by the Miocene and younger Kızılırmak normal fault, with Cappadocian volcanics in its hanging wall (Göncüoğlu *et al.* 1993; Toprak 1994). To the north, the Büyükkışla Formation unconformably overlies metamorphic rocks of the Hırkadağ massif and has a gentle N-dipping stratigraphy (Figure 10a). To the north, this stratigraphy is deformed into the 15 km-wide asymmetric S-vergent 'Killik' syncline (Figure 10b). North of the hinge of the syncline, scattered outcrops in a river valley between Killik and Avuç expose redbeds with gradually steepening S-dipping bedding. Previously, these have been mapped as the Yükseli Formation with volcanic ash deposits with an

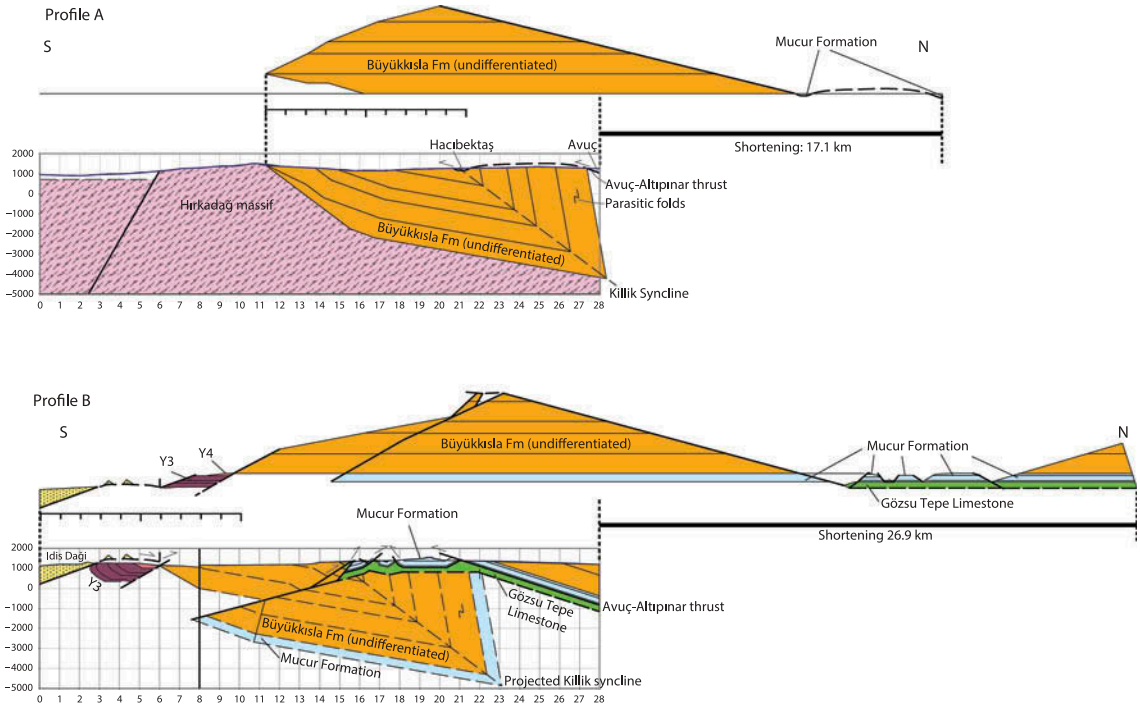


Figure 9. Structural profiles A and B and their restorations. See Figure 4 for locations of the profiles. Büyyükışla Formation and Mucur Formation are not further subdivided into members.

inferred late Miocene–Pliocene age (Atabey 1989), but the gradual steepening bedding and the similarity with lithologies observed in the northern limb led us to interpret this as the Büyükkışla Formation. Subhorizontal thin volcanic ash deposits such as those mapped by Atabey (1989) are indeed present in the map area and are in place preserved as a thin horizontal veneer unconformably covering tilted Büyükkışla Formation rocks. The northern subvertical to slightly overturned limb (Figure 10c), between Hacibektaş, Avuç, and Belbarak, consists of coarse redbed sandstones, with reworked alveolina fossils, derived from the Mucur Formation. This shows that these rocks are not part of the pre-Lutetian Yeşilöz Formation, as previously mapped (Atabey 1989), but of the post-Lutetian Büyükkışla Formation. The northern part of the basin is poorly exposed, but isolated outcrops consistently show subvertical to overturned beddings, with three consecutive outcrops showing opposing younging directions. We interpret this as evidence for parasitic, isoclinal folding in the vertical to slightly overturned limb of the syncline (Figure 9). The syncline is overthrusted southwards along a laterally continuous WNW–ESE trending, NNE-dipping thrust fault (the Avuç–Altıpınar thrust fault, Figures 4 and 9), carrying Eocene limestones and lacustrine series of the Mucur Formation in its hanging wall. In the west of the study area in the village of Hacıbektaş, the hinge of the Killik syncline is overthrusted by basement schists that are unconformably covered by the Eocene Mucur Formation. These schists and Eocene limestones form a klippe (Figure 9). We interpret this klippe as an outlier of the hanging wall of the Avuç–Altıpınar thrust fault system.

The surface trace of the Avuç–Altıpınar thrust fault converges eastwards with the axis of the Killik syncline. Around the village of Sarılar, the northern limb of the syncline is entirely covered by the hanging wall of the Avuç–Altıpınar thrust fault. South of Sarılar, another small klippe of Eocene Mucur limestones overlies the rocks of the southern, N-dipping limb of the Killik syncline. To the east of Büyükkışla, the N-dipping limb of the Killik syncline is further deformed into the northward plunging Sarılar anticline. To the west, this anticline is bordered by a less well-developed syncline, and evidence for E-W shortening disappears westwards. To the east, the Sarılar anticline is bordered by a syncline that is overthrusted with a westward component by essentially non-metamorphosed, folded, and recrystallized ‘Gözsu Tepe’ limestones (Figure 4) with a folded but well-recognizable bedding that appear to be of much lower metamorphic grade than the basement of the Hırkadağ massif. These limestones certainly do not belong to the Ayhan–Büyükkısla stratigraphy (Figure 4). The thrust fault carrying the Gözsu Tepe limestones is at a structurally lower level than the continuous Avuç–Altıpınar thrust fault. The thrust fault at the base of the Gözsu Tepe limestones, directly above the overthrusted Büyükkışla redbeds, exposes a brittle mélange containing intensely brecciated,

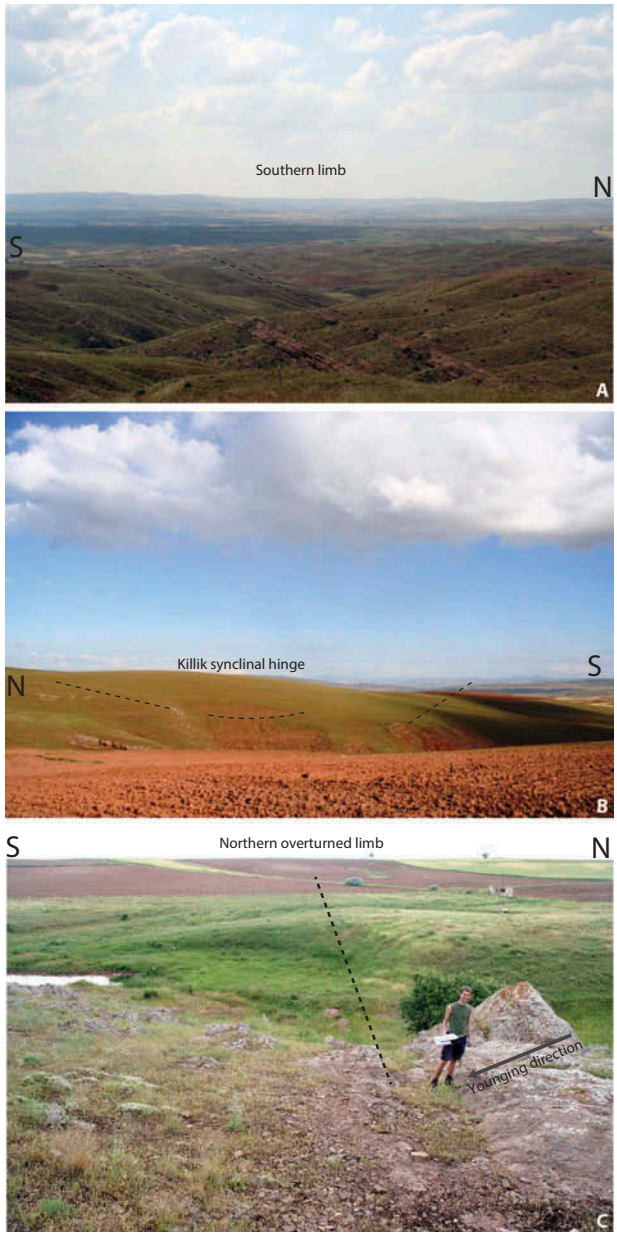


Figure 10. Field photographs of the limbs (a, c) and hinge (b) of the Killik syncline that deformed the Büyükkışla Formation.

foliated marbles, as well as oncolith-bearing limestone blocks exposed in a small quarry southeast of Sarılar.

The surface trace of the thrust fault along the western edge of the Gözsu Tepe limestones disappears to the S. The Gözsu Tepe thrust sheet (Figure 4) dips eastwards, and E of the road from Özkonak to Altıpınar it is unconformably overlain by a several 100 m-thick sequence of lacustrine marls with turbidites and limestones of the Mucur Formation (Member M2). These are deformed by S- and N-dipping thrust faults (profile B of Figure 9). This profile was documented along a well-exposed river valley between Özkonak and Altıpınar (Figure 4). The northern part of this profile is dominated by southward thrust faults, which formed structurally below the Avuç–Altıpınar thrust fault. To the S, however, the dominant thrust direction is northwards. At the southern end of the exposed profile, a thin (~25 m thick) sliver of Gözsu Tepe limestones and brecciated foliated marbles thrust over Mucur Formation marls and turbidites with slump structures. This sliver of Gözsu Tepe limestones, in turn, is overthrusted in the south by Büyükkışla Formation red conglomerates from the southern limb of the Killik syncline (Figure 9). The valley between this river section and the exposures of İdiş Dağı is unexposed, but the red colours of the fields suggest the presence of the Büyükkışla Formation. To the south of the village of Göynük, ~30° N-dipping rocks are exposed to the lower members of the Yeşilöz Formation including mafic volcanics. Towards the S, the bedding becomes steeper, and is overturned near the contact with the metamorphic and igneous rocks above the İdiş Dağı thrust fault, thus forming a major N-vergent footwall syncline. Using the mapped trace of the İdiş Dağı thrust fault combined with the topography, we construct an ~20° S-dipping thrust fault, which becomes subhorizontal to the north. As mentioned before, the thrust fault zone exposes an ~50 m-wide tectonic mélange of hanging wall and footwall rocks.

The structure of the Yeşilöz Formation around Ayhan is more complex than that of the overlying Büyükkışla Formation to the north, as illustrated by Figure 11. Strata in the eastern part of the basin are deformed along E–W striking, N-verging folds, and thrust faults, which can be traced eastwards to the region of Göynük, below the İdiş Dağı thrust fault (Figures 4 and 9). Towards the west, fold and thrust faults disappear, and the bedding strike changes to NNW–SSE. Importantly, the northernmost thrust fault in the Ayhan area, carrying Eocene limestones of the Mucur Formation (Member M1) in its hanging wall, is unconformably covered to the northwest of the village of Ayhan by northward tilted sedimentary rocks of Member B1 of the Büyükkışla Formation. Towards the east, however, limestones of the Mucur Formation (Member M1) are thrusted over the Büyükkışla Formation. Folding and thrust faulting must therefore have started prior to the deposition of the Büyükkışla Formation and must have continued until after its deposition, with the Büyükkışla Formation representing syn-compressional deposits. We illustrate the present-day structure of the basin along two cross-sections C and D (Figures 4, 9, and 11).

In the south of the Ayhan area, an ~E–W trending ridge occurs that exposes Karahıdır volcanics intercalating with sedimentary rocks of the Yeşilöz Formation. In the southwest, this ridge is emplaced northwards along an ~E–W trending thrust fault over rocks of Members Y1 and Y2. To the east, however, this thrust fault steps southwards, thrusting İdiş Dağı syenites over the Karahıdır volcanics. There, Karahıdır volcanic rocks are separated from

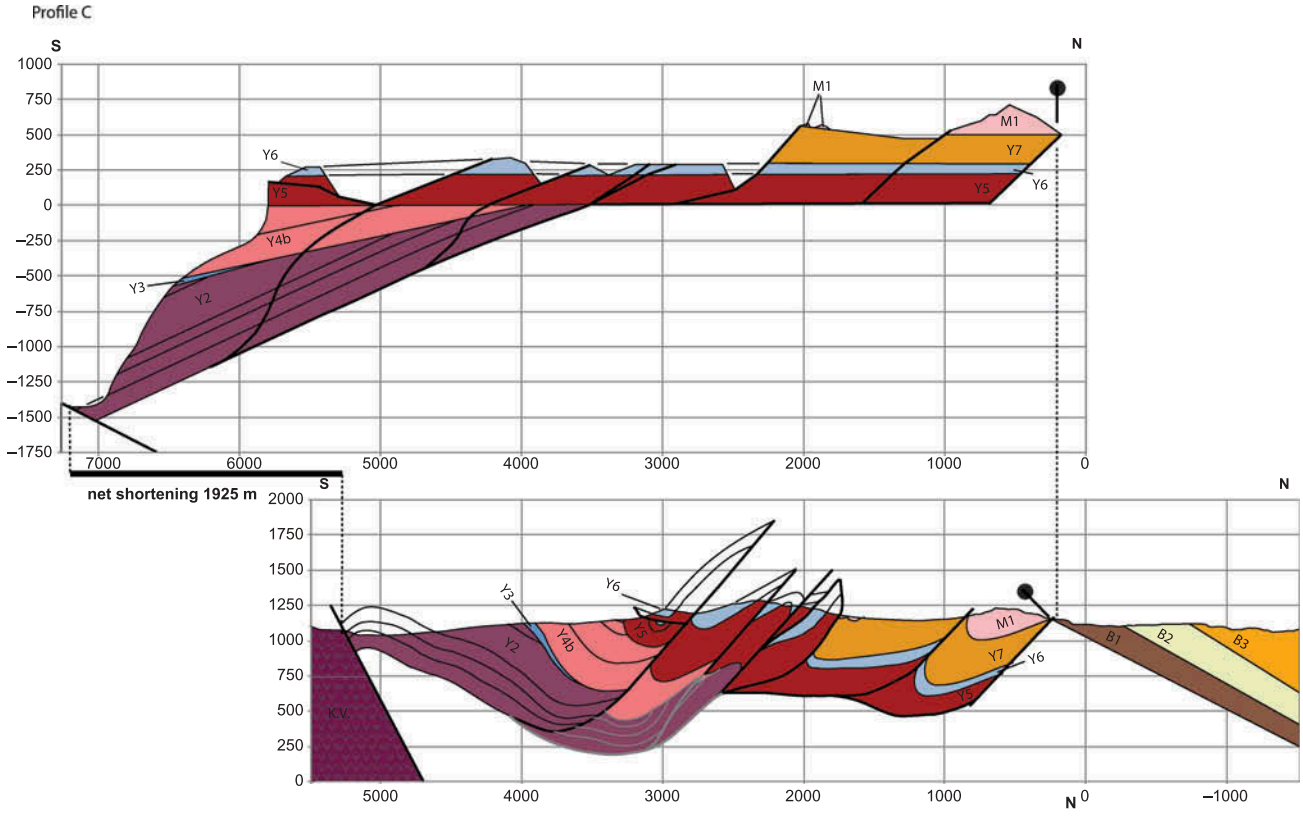


Figure 11. Profile C, across the Ayhan area, and restoration. See Figure 4 for location.

Members Y1 and Y2 by a N-dipping normal fault (Figure 6). Sedimentary rocks of the basal Yeşilöz Formation thicken and taper towards this normal fault, showing it was active during sedimentation (Figure 6). To the south of the ridge of Karahıdır volcanics, red conglomerates and green-yellow sandstones of Members B1 and B2 of the Büyükkışla Formation are found. These dip northwards and are separated from the ridge by a normal fault. We find no evidence of thickening of the Members B1 and B2 towards this normal fault, which suggests that it is a post-sedimentary fault.

Thrust faults and folds dominate the present-day structure of the central and eastern part of the Yeşilöz Formation in the Ayhan area (Figure 12). The eastern profile C (Figure 12) shows the most intensely deformed part. In the south, this profile contains the normal fault between Karahıdır volcanics and Member Y2, and towards the north, a series of N-vergent thrust faults deforms the stratigraphy, associated with a series of hanging wall anticlines and footwall synclines.

The western profile D shows a very different structure. Thrust faults are absent and the cross-section is dominated by NE-ward-tilted beds exposing the entire Yeşilöz Formation. The contact of the sedimentary rocks with the Hırkadağ Massif to the west is a high-angle (up to ~75°) normal fault, described here as the Hüyük Tepe normal fault zone. The Hüyük Tepe normal fault zone comprises two major normal faults in an en-echelon configuration connected via a relay ramp (Figure 4). The presence of young travertine deposits suggests that these faults have experienced some recent activity (Göncüoğlu *et al.* 1993).

To the east of the Hüyük Tepe fault, beds of Member Y2 show drag folding along the normal fault, with bedding orientations that turn near parallel (up to ~75°) to the fault plane. The strike of the bedding of the basal Yeşilöz Formation is oblique to the strike of the Hüyük Tepe fault, striking ~20° more westerly than the fault. Away from the fault, beds of Member Y2 are mildly folded, with bedding first decreasing to an ~20° NE-dipping orientation, followed by steepening to ~50° below an angular unconformity with Member Y3. The angular relationship between Members Y2 and Y3 varies along this unconformity, with a steeper NE-ward tilt of the lower member in the north, and a shallower tilt in the S. We will discuss the implication of this relationship in the next section.

The Hüyük Tepe fault, which must have a vertical displacement equivalent to at least the total stratigraphic thickness of the Yeşilöz Formation, i.e. ~3–4 km, cannot be traced into the Büyükkışla Formation. Although the direct contact of the Büyükkışla Formation and the Hüyük Tepe fault cannot be observed due to lack of exposure, we note that both the northeastward-tilted

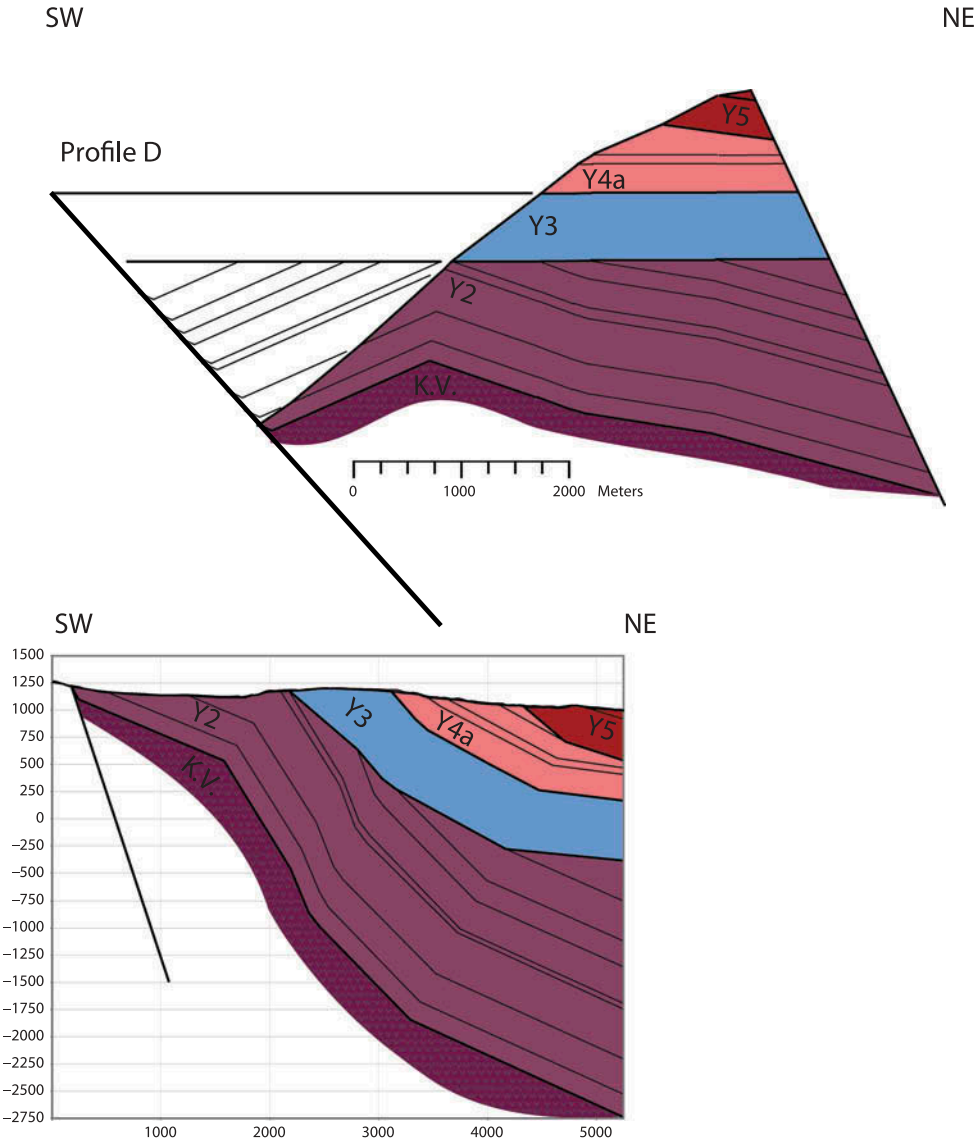


Figure 12. Profile D, and restoration to Member Y3, showing a hanging wall anticline–syncline pair in Member Y2. See Figure 4 for location.



western exposures of the Yeşilöz Formation and the Hırkadağ basement are unconformably covered by the Büyükkışla Formation. There is no evidence for a major normal fault within the Büyükkışla Formation along the northeastward projection of the Hüyük Tepe fault. The bulk of Hüyük Tepe fault displacement therefore predates the deposition of the Büyükkışla Formation.

### 5.2. *Restoring post-middle Eocene shortening*

To quantify the amount of post-middle Eocene shortening in the study area, and to restore the Yeşilöz Formation in its configuration at the inception of folding, we have restored the cross-sections A–D described above (Figures 9, 11, and 12). Cross-section restoration was performed via line-length balancing, using the sinuous bed method of Dahlstrom (1969). The deformed state cross-section is constructed assuming parallel folding for folds directly related to faulting (such as the Hüyük Tepe hanging wall syncline and the Killik footwall syncline). For these folds, the axial plane is roughly parallel to the fault. For folds that are not directly related to faulting, concentric folding is assumed. The hinge planes are constructed parallel to the bisectrix of two bedding planes, according to the methods of Suppe (1983). In the restoration, conservation of area (Dahlstrom 1969) is applied. All cross-sections are solely based on interpretations of the surface geology. The section is restored to the base of the Büyükkışla Formation.

Based on the surface geology, the subvertical northern limb of the Killik syncline appears to be thicker than the southern limb. Here we consider two possible end-member scenarios for this thickening. In the first scenario, thickening is assumed to be the result of a northward increase in stratigraphic thickness, and no shortening in the north limb is assumed.

In the second scenario, thickening is assumed to be tectonic in nature, caused by shortening of the northern limb by isoclinal folding. In cross-section A (Figure 9), the hinge (fold axial) plane of the Killik syncline is more or less planar, which results in a thickened northern limb. This may be due to tectonic thickening, consistent with the evidence for meso-scale isoclinal folding. In the restoration, the northern limb is thinned to the same thickness as the southern limb. To conserve volume, the northern limb is elongated in the restored section. To construct the lower part of cross-section B (İdiş Dağı–Altıpınar), cylindrical folding of the Killik syncline is assumed. This syncline is projected into this cross-section. Here, we also consider the two possible end-member scenarios.

Balanced sections A and B provide minimum shortening estimates between ~40% and ~50% (between 14.5–17.1 km and 24.3–26.9 km of shortening, respectively, Figure 9). Restoration of cross-section C across the Yeşilöz Formation to the East of Ayhan reveals a minimum shortening of ~2 km (~30%) (Figure 11). Because the western part of the basin has no significant shortening component, this part of the basin is most likely close to the pre-compressional orientation of the basin relative to the Hırkadağ massif. If we correct for the eastward increasing shortening using the estimate of profile C, it follows that the E–W trend of the central and eastern part of the Ayhan basin is the result of a shortening-related, local counterclockwise vertical axis rotation around a pole in the southwest of the basin.

In its pre-compressional configuration, the N-dipping normal fault in the southeast of the Ayhan basin (i.e. at the southern end of profile C) would rotate backwards into a flat-lying structure with a top-to-the-NE sense of shear. Restoring the basin to Member Y5 reveals that the intrabasinal angular unconformities between Members Y2 and Y3 and Y4 and Y5 result from progressive SW-ward tilting of the stratigraphy towards the normal fault in the south of the profile (Figure 11). This is consistent with evidence for syn-sedimentary tapering of Member Y2 adjacent to the fault (Figure 6) and shows that the Ayhan basin, during deposition until at least Member Y5, was extensional.

We also restore section D into its pre-compressional configuration. Although this section underwent only minor internal deformation during the compression episode, the unconformably covering Büyükkışla redbeds are consistently tilted by ~35° to the north. Part of this tilt might result from footwall uplift associated with the upper Miocene and younger normal faults to the south of the Hırkadağ massif and south of the Ayhan basin, and in part might be due to loading along the Avuç–Altıpınar thrust fault. Correcting the bedding measurements from the western Ayhan basin for this tilt leads to a decrease of the dip of the Hüyük Tepe normal fault to ~50°, and the corrected strike of the Ayhan bedding is oriented parallel to the Hüyük Tepe fault. This strengthens the interpretation that the Hüyük Tepe normal fault predates the Büyükkışla redbeds and their tilting and governed at least part of the deposition of the Ayhan basin stratigraphy.

## 6. Discussion

### 6.1. *Post-mid-Eocene Savcılı thrust zone accommodating block rotations*

Our results demonstrate that after Lutetian deposition of the Mucur Formation, and during (or before and after) the deposition of the Büyükkışla Formation, the Ayhan–Büyükkışla basin was shortened by ~40–50%, over a minimum amount of 24–27 km in section B (Figure 9). We will discuss below the implications of this finding for the role of the fault zone that was postulated to accommodate relative vertical axis rotations between the Kırşehir and Niğde-Ağaçören massifs of the CACC (Lefebvre *et al.* 2013). First, however, we discuss the complicated structure to the northeast of Büyükkışla around Sarılar (Figure 4), where N–S trending, N-plunging anticlines, and synclines overprint the Kilik syncline to the west of the Gözsu Tepe limestone thrust sheet.

The Gözsu Tepe thrust fault has a lower structural level than Avuç–Altıpınar thrust fault (Figure 9) and brings deeper rocks of the tectonostratigraphy to the surface. We interpret the western faulted boundary of the Gözsu Tepe limestone sheet as essentially a sidewall ramp. The Mucur Formation lacustrine sequences (Member M2) unconformably overlying the Gözsu Tepe limestones are not only overthrusted from the N, but also from the S, where in profile B we find Gözsu Tepe limestones and associated brecciated foliated marble thrusting northwards over Member M2 (Figure 9). We therefore explain the N–S trending Sarılar anticline and the westward thrust fault of the Gözsu Tepe limestones over the Büyükkışla redbeds to result from a small and local counterclockwise rotation of the Gözsu Tepe thrust sheet around a pivot point in the south, where southward motion of the thrust sheet is blocked by top-to-the-N thrust faults. Such a minor counterclockwise rotation would induce a local space problem in the area of Sarılar, inducing an E–W-directed component of shortening on the Gözsu Tepe sidewall ramp that formed the observed thrust faulting and folding (Figure 13). We consider this deformation of only local importance and focus on the N–S shortening component in the remainder of this discussion.

Lefebvre *et al.* (2013) postulated that the palaeomagnetically documented 29.0 ± 4.5° rotation difference

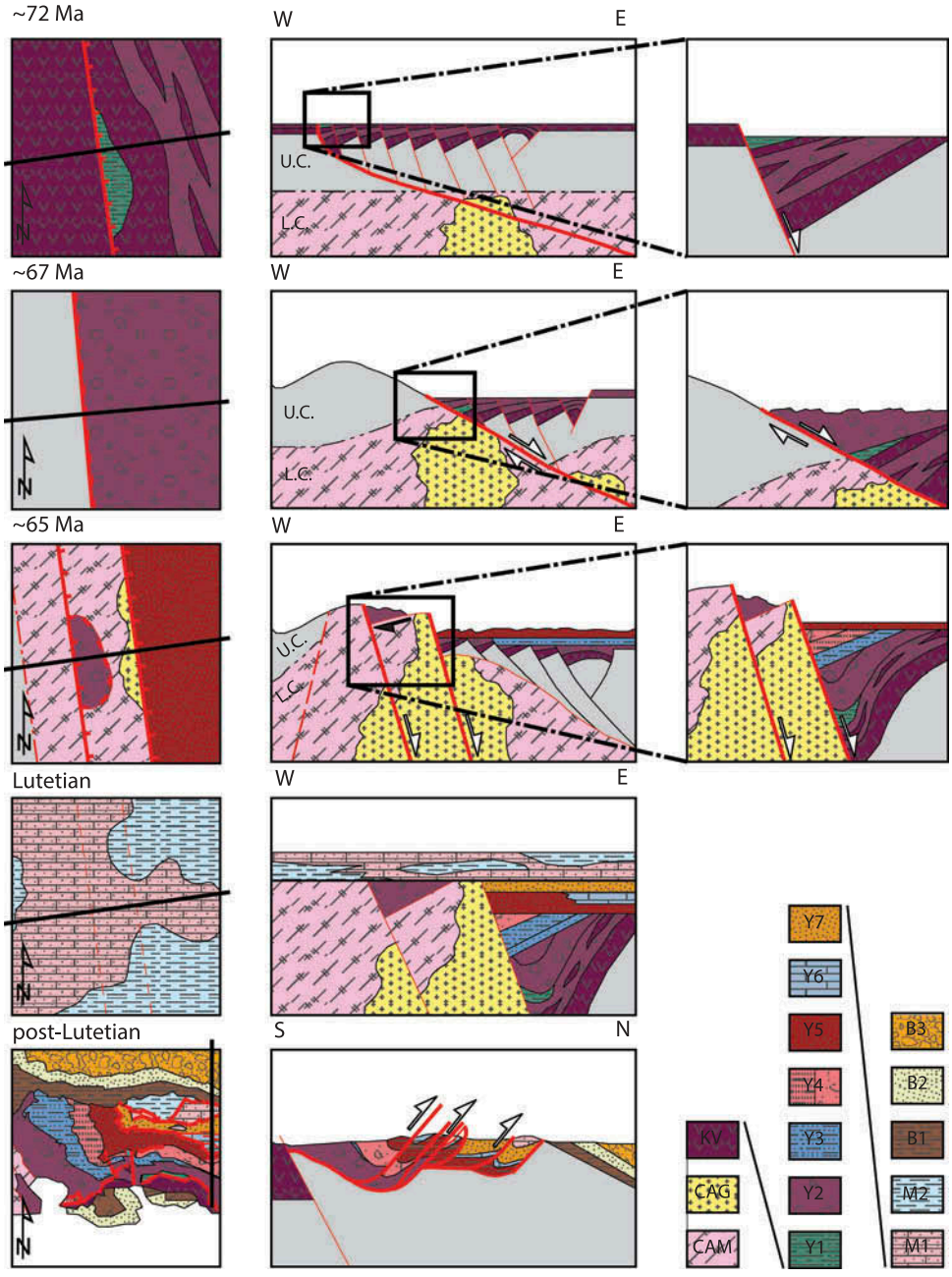


Figure 13. Schematic evolution of the Ayhan–Büyükkışla basin. In Late Cretaceous time (at least 72–66 Ma), the basin evolved as a supradetachment basin above the originally top-to-the-E Hırkadağ detachment. Subsequently, during the late stages of exhumation, the high-angle Hüyük Tepe normal faults cut the detachment and governed deposition of the upper part of the Yeşilöz Formation. Regional (at least CACC-wide) Lutetian transgression led to the deposition of the Mucur Formation, unconformably overlying all older units. Post-Lutetian and pre-late Miocene compression in the Ayhan–Büyükkışla basin accommodated ~30° of counterclockwise vertical axis rotation of the Niğde–Ağaçören massif relative to the Kırşehir Massif (Lefebvre *et al.* 2013). Finally (not indicated), the late Miocene and younger Kızılırmak normal fault subsided the Cappadocia volcanic province to the south relative to the Ayhan–Büyükkışla–Hırkadağ region to the north.

between the Kırşehir and Niğde–Ağaçören massifs was accommodated in the Savcılı thrust zone between the Hırkadağ massif and the Kırşehir massif (Figures 2 and 3). This would require ~40–60 km of N(NE)–S(SW) shortening to be accommodated within the Savcılı thrust zone, alongside a relatively minor (~10 km) left-lateral strike-slip component.

Accommodating this shortening in the ~30 km-wide zone between Hırkadağ and Kırşehir massifs, the southern part of which is occupied by the Ayhan–Büyükkışla basin,

would require ~50–65% shortening. This is reasonably consistent with the ~50% shortening we restored in section B, but requires that the poorly exposed valley between the Avuç–Altıpınar thrust fault and the Mucur massif (Figure 2) underwent similar or somewhat higher shortening. This valley is too poorly exposed to map in detail, but scarce outcrops expose steeply tilted redbeds and Mucur Formation limestones, suggesting that the fold–thrust zone extends further northwards than our study area. Given the similarity between the restored shortening percentages in the Ayhan–Büyükkışla basin and the predicted values for the Savcılı thrust zone by Lefebvre *et al.* (2013), we consider their hypothesis viable that the Kırşehir and Niğde–Ağaçören massifs represent more or less rigid blocks in Cenozoic time, whose relative rotation is accommodated in the Savcılı thrust zone.

Our documentation shows that the age of the shortening in the Ayhan–Büyükkışla basin is post-Lutetian, which also constrains the age of the block rotation between the Kırşehir and Niğde–Ağaçören massifs as younger than the Lutetian. Kaymakcı *et al.* (2009), Meijers *et al.* (2010), and Lefebvre *et al.* (2013) argued that deformation of the Pontides and Central Anatolian compression started shortly after the initiation of collision of the CACC with the Pontides in the Palaeocene. Our finding suggests that the compressional deformation and block rotations of central Anatolia occurred during a protracted period of time. This is consistent with evidence for late Eocene (~39–35 Ma) N–S shortening in the Çiçekdağı basin (Gülyüz *et al.* 2013) and contraction in the Çankırı basin continuing into Oligocene time (Kaymakcı *et al.* 2009) and late Eocene or younger shortening in the Ulukışla basin to the south of the CACC (Clark and Robertson 2005). Shortening must be older than the formation of the N–S extensional Kızılırmak normal fault, which presumably occurred in late Miocene time. To the south of the CACC, the Adana basin records early Miocene ~NW–SE extension in the forearc of the Cyprus subduction zone, suggesting that since this time the overriding plate is in (mild) extension (Aksu *et al.* 2005; Burton-Ferguson *et al.* 2005); central Anatolian N–S shortening and block rotations, being governed by Africa–Europe convergence, most likely ended before the early Miocene.

### 6.2. *Late Cretaceous extension: relation to the exhumation of the CACC metamorphics?*

During the inception of sedimentation, at least 72.11 ± 1.46 million years ago as shown by our dating of a lava at the base of the stratigraphy (Figure 8), the Ayhan–Büyükkışla basin was an extensional basin. This is shown by the intra-basinal syn-sedimentary normal fault separating the ridge of Karahıdır volcanics from higher parts of Member Y2 of the Yeşilöz Formation in the southeastern part of the Ayhan area (Figures 4 and 6c), the intra-basinal unconformities that result from southward tilting of the stratigraphy towards this fault (Figure 11), and smaller syn-sedimentary normal faults preserved within the Yeşilöz Formation (Figure 6b). In addition, our mapping of the stratigraphy in the hanging wall of the Hüyük Tepe normal fault shows an intraformational unconformity between Members Y2 and Y3, the lower unit being folded as a hanging wall syncline–anticline pair consistent with activity of the Hüyük Tepe normal fault. Restoring the orientation of the presently top-to-the-NE Hüyük Tepe normal fault for the ~35° counterclockwise vertical axis rotations recorded in the Ağaçören plutons (Lefebvre *et al.* 2013) (Figure 3) suggests that Late Cretaceous extension direction was E–W directed.

On a regional scale, exhumation of the CACC occurred until ~65–60 Ma (Boztuğ and Jonckheere 2007; Boztuğ *et al.* 2007, 2009b; Gautier *et al.* 2008; Isik *et al.* 2008; Isik 2009; Lefebvre 2011; Lefebvre *et al.* 2011), i.e. contemporaneous with the early stages of sedimentation of the Ayhan–Büyükkışla basin. Where documented, extension directions of syn-exhumation shear zones, corrected for vertical axis rotations, also indicate an E–W extension direction. We therefore postulate that the extension documented in the Ayhan–Büyükkışla basin is associated with regional exhumation of the CACC metamorphics.

Lefebvre (2011) documented in the eastern part of the Hırkadağ massif a ductile-to-brittle, top-to-the-NE extensional detachment, separating conglomerates that are similar in colour and detrital content to Member Y2 from exhumed basement. Lefebvre (2011) dated a granodiorite in the Hırkadağ massif with U/Pb on zircon at 77.30 ± 0.39 Ma and obtained biotite and K-feldspar cooling ages of an amphibolite sample from the Hırkadağ massif of 68.8 ± 1.4 Ma and 67.0 ± 1.2 Ma (Figure 5), respectively, showing that the Hırkadağ basement was not yet at the surface when sedimentation in the Ayhan–Büyükkışla basin commenced. This is consistent with the absence of metamorphic and granitic debris in the lower Members (Y1–Y2) of the basin's stratigraphy. The early stages of the basin's history, at least during the deposition of Members Y1 and Y2, may thus be viewed as a supradetachment basin setting. The Hüyük Tepe normal faults may then be explained as high-angle normal faults within the same extensional system that cut the back-tilted detachment at a late stage during the exhumation history. An analogue may be formed by the by the upper Miocene–Pliocene Alaşehir and Büyük Menderes detachment faults in the Menderes Massif of western Turkey, where a lower to middle Miocene supradetachment basin stratigraphy (Şen and Seyitoğlu 2009; Oner and Dilek 2011, 2013) was crosscut by high-angle normal faults in the late stages of extension following the bulk of exhumation of the underlying metamorphic rocks, followed by continued deposition in the Büyük Menderes

and Gediz grabens (Bozkurt 2000; Çiftçi and Bozkurt 2009, 2010; Gürer *et al.* 2009; Çifçi *et al.* 2011). A similar evolution of low- to high-angle normal faulting governing sedimentation during exhumation is typical for supradetachment basins across the eastern Mediterranean (Sanchez-Gomez *et al.* 2002; van Hinsbergen and Meulenkamp 2006; Cavazza *et al.* 2009; Zachariasse *et al.* 2011).

### 6.3. *Implications for the Cretaceous subduction configuration of Central Anatolia*

Based on the distribution of the plutons in the CACC with geochemistries inferred to reflect arc volcanism (Ilbeyli 2005; Kadıoğlu *et al.* 2006) and the presence of contemporaneous HP-LT metamorphic rocks to the west of the CACC (e.g. Okay *et al.* 1996; Pourteau *et al.* 2010; Whitney *et al.* 2011), Lefebvre *et al.* (2013) suggested that in Late Cretaceous time the CACC was located above an E-dipping subduction zone that created E–W overriding plate extension. The Late Cretaceous E–W restored extension direction of the Ayhan–Büyükkışla basin (Figure 3) is consistent with this reconstruction. As discussed above, compression in the Ayhan–Büyükkışla basin occurred during central Anatolian deformation that Lefebvre *et al.* (2013) related to the collision of the CACC with the Pontides after the arrest of oceanic subduction of Neotethyan oceanic lithosphere below the Pontides.

During the Late Cretaceous, (at least) two subduction zones must have been active in the Eastern Mediterranean region, as has been frequently postulated before (e.g. Moix *et al.* 2008). Our kinematic analyses confirm the reconstructions of Lefebvre *et al.* (2013) that argue that the intra-Tauride subduction zone to the west of the CACC was ~N–S striking and must thus have been highly oblique.

Our study is only a first step into a quantitative kinematic restoration of the Cretaceous subduction configuration of Turkey, and future work should further quantify shortening, extension, and rotation in the Tauride fold–thrust belt and the Tuz Golu and Sivas Basins. In Figure 14, however, we provide one possible subduction zone geometry and evolution for the Eastern Mediterranean region during Cretaceous to Eocene time in Figure 14 that fulfils the constraints provided in this article, those for western Turkey and the Aegean region summarized in reconstructions of van Hinsbergen *et al.* (2005, 2010), van Hinsbergen and Schmid (2012), and Gaina *et al.* (2013), and for eastern Anatolia as summarized by Pourteau *et al.* (2010).

A northern, E–W trending, N-dipping subduction zone existed below the Pontides and had been active since at least Early Cretaceous time (Okay *et al.* 2013). Westwards, this subduction zone connected to the subduction zone along the southern Rhodope that had existed since at least some 100 million years ago (van Hinsbergen *et al.* 2005; Jolivet and Brun 2010). To the south of the Pontides, Cretaceous ophiolites are found in tectonic contact above all tectonic units of the Taurides, the Afyon

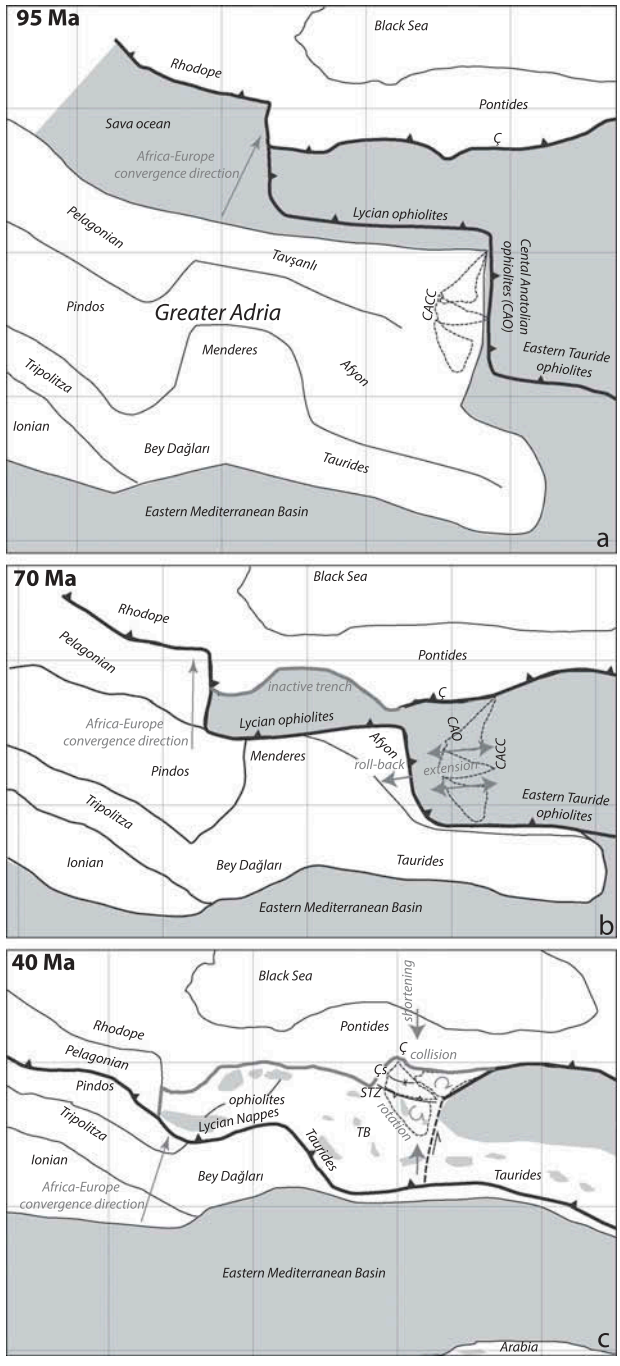


Figure 14. Schematic plate boundary configuration for the eastern Mediterranean region at (a) 95 Ma, corresponding to the period of subduction initiation below the Anatolian ophiolites; (b) 70 Ma, corresponding to the period of arc magmatism and E–W extension in the CACC, and (c) 40 Ma, corresponding to the period of block rotation and N–S contraction in central Anatolia. Graticules are in 5° latitude and longitude intervals.

zone, the Tavşanlı zone, and the CACC (e.g. Dilek and Furnes 2009). Where metamorphic soles are found below the Anatolian ophiolites, these are ~90–95 million years old (Çelik *et al.* 2006), which is widely interpreted to shortly post-date initiation of a subduction zone below the oceanic lithosphere of which these ophiolites are relics (e.g. Isik *et al.* 2008; Isik 2009; Sarıfakıoğlu *et al*. 2013). Shortly after subduction initiation, continental crust was underthrusted in western Turkey (the lower nappes of the Tavşanlı zone, Plunder *et al*. 2013) and in central Turkey (CACC) (e.g. Boztuğ *et al.* 2009b). The 85 Ma and even older, undeformed granitoids that intrude the CACC and overlying central Anatolian ophiolites demonstrate that within 10 million years after subduction initiation, rocks of the CACC had been underthrusted below and accreted to the overlying oceanic lithosphere. When corrected for Cenozoic rotations (Lefebvre *et al.* 2013), an intense and persistent NNE–SSW-trending, syn-regional metamorphic stretching lineation on shallowly inclined pervasive foliation associated with top-to-the-SSW sense of shear is prominent across the entire CACC (Lefebvre 2011). These deformation fabrics predate granitoid intrusion and are parallel and hence likely the result of the north-northeastward underthrusting of the CACC below the central Anatolian ophiolites.

The palaeomagnetic reconstruction of Lefebvre *et al.* (2013) shows that the CACC had a N–S lenticular orientation after its underthrusting below and accretion to the central Anatolian ophiolites, and became intruded by a N–S-trending volcanic arc. Consequently, those authors inferred that a N–S-trending subduction segment must have existed in central Anatolia. The widespread presence of ophiolites in western Turkey shows that an intra-oceanic subduction zone must also have been present in western Turkey, and reconstructions of van Hinsbergen *et al.* (2010) and Plunder *et al.* (2013) advocate that this intra-oceanic subduction zone was E–W trending. Similarly, a roughly E–W-trending intra-oceanic subduction zone is required north of the eastern Taurides to allow regional ophiolite emplacement there. We hence suggest that a strongly curved or discretely segmented Late Cretaceous subduction zone existed in central Anatolia, with a highly oblique N–S-trending subduction segment below which the CACC became underthrusted. This geometry may be comparable to the margin of Tibet and Sundaland, with a highly oblique N–S-trending subduction zone along the Birma block and the Andaman Sea connecting sub-orthogonal E–W-trending subduction zones of southern Tibet and Sumatra-Java (e.g. Hall 2002, 2012; van Hinsbergen *et al.* 2011).

Extensional shear zones and detachments in the CACC (Gautier *et al.* 2008; Isik *et al.* 2008; Isik 2009; Lefebvre 2011; Lefebvre *et al.* 2011, 2012) and the early stages of infill of the Ayhan basin demonstrate that the CACC was affected and exhumed by E–W extension in latest Cretaceous time. Arc magmatism remained active during this stage (e.g. Lefebvre 2011; Lefebvre *et al.* 2011; and this paper) and subduction occurred westwards of the CACC, burying the Afyon zone (e.g. Pourteau *et al.* 2010, 2013). E–W extension in the overriding plate that exhumed the CACC then likely reflects westward trench retreat of the N–S-striking central Anatolian subduction segment.

Around 65 Ma, the CACC and overlying ophiolites collided with the Pontides as a result of ongoing convergence accommodated by the northern subduction zone. This collision initiated a phase of N–S shortening in central Anatolia causing the formation of a northward convex orocline (Meijers *et al.* 2010) and intense thrusting in the central Pontides (Espurt *et al.* 2014) and the Çankırı Basin (Kaymakci *et al.* 2003, 2009). To the south, N–S contraction led to the break-up of the CACC into three massifs that rotated and moved relative to each other (Lefebvre *et al.* 2013), reflected by Eocene to Oligocene folding and thrust faulting in the Savcılı thrust zone (Isik *et al.* 2014) and the Ayhan–Büyükkişla Basin (this study), the Çiçekdağı basin (Gülyüz *et al.* 2013), and to the south, in the Ulukışla Basin (Görür *et al.* 1998; Clark and Robertson 2005). During the later stages of this episode, ongoing N–S convergence to the east of the CACC became accommodated by the Ecemiş left-lateral strike-slip fault at its eastern border (Jaffrey and Robertson 2001). To the west and south, the Taurides were accreted structurally below the Afyon zone, which became widely exhumed in central and western Turkey, perhaps as a result of ongoing trench retreat of the central Anatolian subduction zone segment. We tentatively postulate that a relict of the N–S striking, E-dipping slab that dominated the Cretaceous evolution of the CACC may still exist today: such a feature is imaged by seismic tomography below the modern Isparta Angle in southwest Anatolia (de Boorder *et al.* 1998; Biryol *et al.* 2011).

## 7. Conclusions

The CACC underwent Late Cretaceous regional Barrovian metamorphism following ophiolite obduction. Previously documented extensional detachment histories suggest that extensional exhumation occurred until latest Cretaceous times. This was followed by latest Cretaceous to Palaeocene inception of collision of the CACC with the Pontides. Recent palaeomagnetic data (Lefebvre *et al.* 2013) demonstrated that the CACC was subsequently fragmented into three massifs (Akdağ, Kırşehir, and Niğde-Ağaçören massifs), which rotated relative to each other. In this study, we test whether an ~30° vertical axis rotation difference between the Kırşehir and Niğde–Ağaçören massifs may have been accommodated by ~40–60 km of shortening (50–65%) in the region between the Hırkadağ massif in the south (belonging to the Niğde–

Ağaçören massif) and the Mucur massif in the north (belonging to the Kırşehir massif).

We studied the Upper Cretaceous to post-middle Eocene Ayhan–Büyükkışla basin, located adjacent to the Hırkadağ massif in the central part of the CACC. The basin is subdivided into three formations, based on their stratigraphy and structure, each of which represents subsequent stages in the tectonic evolution of the basin. The results of this study show that the Ayhan–Büyükkışla basin records both Late Cretaceous extension and post-middle Eocene (Lutetian) compression.

Deposition started in an extensional basin around 72.11 ± 1.46 ($^{40}Ar/^{39}Ar$ plagioclase age on andesite at the base of the stratigraphy). Restored for post-Cretaceous rotations, we restore an E–W extension direction, consistent with regional constraints. The extensional basin sedimentary rocks were unconformably covered by mid-Eocene limestones and redbeds, followed by intense folded and thrust faulting. Two balanced cross-sections in the study area give ~50% of post-mid-Eocene ~N–S shortening, consistent with the predicted value from the rotation analysis. We thus confirm predictions of a palaeomagnetism-based reconstruction of central Anatolia, which implied that the well-documented Late Cretaceous intra-Tauride subduction zone to the west of the CACC was N–S-striking and E-dipping, creating E–W extension in the overriding plate. Given Africa–Europe convergence directions at that time, this subduction zone must have been highly oblique. Our study is a first step towards quantitative kinematic restorations of subduction zone configurations and evolution of the Eastern Mediterranean in Cretaceous time.

## Acknowledgements

We thank Demir Altıner, Rob Scaife, Henk Brinkhuis, and Appy Sluijs for analysing samples for fossil content (which unfortunately were barren). Maarten Zeylmans-van Emichoven is thanked for his assistance with the GIS software. We thank Paul Umhoefer and an anonymous reviewer for constructive comments.

## Funding

E.L.A. acknowledges the funding from the Molengraaff Foundation. E.L.A., R.L.M.V., and N.K. acknowledge the financial support from the Darius Foundation. D.J.J.v.H. was supported by ERC Starting Grant 306810 (SINK) and a Dutch Science Council VIDI grant.

## References

Aksu, A.E., Calon, T.J., Hall, J., Mansfield, S., and Yaşar, D., 2005, The Cilicia–Adana basin complex, Eastern Mediterranean: Neogene evolution of an active fore-arc basin in an obliquely convergent margin: Marine Geology, v. 221, p. 121–159. doi:10.1016/j.margeo.2005.03.011

Atabey, E., 1989, Kayseri - H19 Paftası Jeoloji Haritası: Ankara, Turkey, General Directorate of Mineral Research and Exploration (MTA) Publication.

Aydın, N., 1985, Geological evolution of Gümüşkent town and it's surrounding in the Middle Anatolian Massif, Communications: de La Faculté des Sciences de l'Université d'Ankara, série C1 Géologie, v. 31, p. 43–56.

Barrier, E., and Vrielynck, B., 2008, MEBE Atlas of Paleotectonic maps of the Middle East: Commission for the Geological Map of the World, v. 14.

Biryol, C.B., Beck, S.L., Zandt, G., and Özacar, A.A., 2011, Segmented African lithosphere beneath the Anatolian region inferred from teleseismic P-wave tomography: Geophysical Journal International, v. 184, p. 1037–1057. doi:10.1111/j.1365-246X.2010.04910.x

Bozkurt, E., 2000, Timing of extension on the Büyük Menderes Graben, western Turkey, and its tectonic implications, in Tectonics and Magmatism in Turkey and the Surrounding Area, *in* Bozkurt, E., Winchester, J.A., and Piper, J.D.A., eds., Geological Society, London, Special Publication, v. 173, p. 385–403.

Boztuğ, D., Güney, Ö., Heizler, M., Jonckheere, R.C., Tichomirowa, M., and Otlu, N., 2009a, $^{207}Pb$-$^{206}Pb$, $^{40}Ar$-$^{39}Ar$ and fission-track geothermochronology quantifying cooling and exhumation history of the Kaman-Kirsehir region intrusions, Central Anatolia, Turkey: Turkish Journal of Earth Sciences, v. 18, p. 85–108.

Boztuğ, D., and Jonckheere, R.C., 2007, Apatite fission track data from central Anatolian granitoids (Turkey): Constraints on Neo-Tethyan closure: Tectonics, v. 26, p. TC3011. doi:10.1029/2006TC001988

Boztuğ, D., Jonckheere, R.C., Heizler, M., Ratschbacher, L., Harlavan, Y., and Tichomirova, M., 2009b, Timing of post-obduction granitoids from intrusion through cooling to exhumation in central Anatolia, Turkey: Tectonophysics, v. 473, p. 223–233. doi:10.1016/j.tecto.2008.05.035

Boztuğ, D., Tichomirowa, M., and Bombach, K., 2007, $^{207}Pb$-$^{206}Pb$ single-zircon evaporation ages of some granitoid rocks reveal continent-oceanic island arc collision during the Cretaceous geodynamic evolution of the central Anatolian crust, Turkey: Journal of Asian Earth Sciences, v. 31, p. 71–86. doi:10.1016/j.jseaes.2007.04.004

Burton-Ferguson, R., Aksu, A.E., Calon, T.J., and Hall, J., 2005, Seismic stratigraphy and structural evolution of the Adana Basin, eastern Mediterranean: Marine Geology, v. 221, p. 189–222. doi:10.1016/j.margeo.2005.03.009

Cavazza, W., Okay, A.I., and Zattin, M., 2009, Rapid early-middle Miocene exhumation of the Kazdağ Massif (western Anatolia): International Journal of Earth Sciences, v. 98, p. 1935–1947. doi:10.1007/s00531-008-0353-9

Çelik, Ö.F., Delaloye, M.F., and Feraud, G., 2006, Precise 40Ar–39Ar ages from the metamorphic sole rocks of the Tauride Belt Ophiolites, southern Turkey: Implications for the rapid cooling history: Geological Magazine, v. 143, p. 213–227. doi:10.1017/S0016756805001524

Çifçi, G., Pamukçu, O., Çoruh, C., Çopur, S., and Sözbilir, H., 2011, Shallow and deep structure of a supradetachment basin based on geological, conventional deep seismic reflection sections and gravity data in the Buyuk Menderes Graben, western Anatolia: Surveys in Geophysics, v. 32, p. 271–290. doi:10.1007/s10712-010-9109-8

Çiftçi, N.B., and Bozkurt, E., 2009, Evolution of the Miocene sedimentary fill of the Gediz Graben, SW Turkey: Sedimentary Geology, v. 216, p. 49–79. doi:10.1016/j.sedgeo.2009.01.004

Çiftçi, N.B., and Bozkurt, E., 2010, Structural evolution of the Gediz Graben, SW Turkey: Temporal and spatial variation of the graben basin: Basin Research, v. 22, p. 846–873.

Clark, M., and Robertson, A.H.F., 2005, Uppermost Cretaceous–Lower Tertiary Ulukışla Basin, south-central Turkey: Sedimentary evolution of part of a unified basin complex within an evolving Neotethyan suture zone: Sedimentary Geology, v. 173, p. 15–51. doi:10.1016/j.sedgeo.2003.12.010

Dahlstrom, C.D.A., 1969, Balanced cross-sections: Canadian Journal of Earth Sciences, v. 6, p. 743–757. doi:10.1139/e69-069

de Boorder, H., Spakman, W., White, S.H., and Wortel, M.J.R., 1998, Late Cenozoic mineralization, orogenic collapse and slab detachment in the European Alpine Belt: Earth and Planetary Science Letters, v. 164, p. 569–575. doi:10.1016/S0012-821X(98)00247-7

Dercourt, J., Zonenshain, L.P., Ricou, L.-E., Kazmin, V.G., Le Pichon, X., Knipper, A.L., Grandjacquet, G.C.,.I.M., Sbortshikov, I.M., Geyssant, J., Lepvrier, C., Pechersky, D. H., Boulin, J.-C., Sibuet, J., Savostin, L.A., Sorokhtin, O., Westphal, M.L., Bazhenov, M.L., Lauer, J.P., and Biju-Duval, B., 1986, Geological evolution of the Tethys Belt from the Atlantic to the Pamirs since the Lias: Tectonophysics, v. 123, p. 241–315. doi:10.1016/0040-1951(86)90199-X

Dilek, Y., and Altunkaynak, Ş., 2007, Cenozoic crustal evolution and mantle dynamics of post-collisional magmatism in western Anatolia: International Geology Review, v. 49, p. 431–453. doi:10.2747/0020-6814.49.5.431

Dilek, Y., and Altunkaynak, S., 2009, Geochemical and temporal evolition of Cenozoic magmatism in western Turkey: Mantle response to collision, slab breakoff, and lithospheric tearing in an orogenic belt, *in* van Hinsbergen, D.J.J., Edwards, M. A., and Govers, R., eds., Geodynamics of collision and collapse at the Africa-Arabia-Eurasia subduction zone: Geological Society of London Special Publication, v. 311, p. 213–234.

Dilek, Y., and Furnes, H., 2009, Structure and geochemistry of Tethyan ophiolites and their petrogenesis in subduction rollback systems: Lithos, v. 113, p. 1–20. doi:10.1016/j.lithos.2009.04.022

Dilek, Y., and Sandvol, E., 2009, Seismic structure, crustal architecture and tectonic evolution of the Anatolian-African Plate Boundary and the Cenozoic Orogenic Belts in the Eastern Mediterranean Region: Geological Society, London, Special Publications, v. 327, p. 127–160. doi:10.1144/SP327.8

Dilek, Y., Thy, P., Hacker, B.R., and Grundvig, S., 1999, Structure and petrology of Tauride ophiolites and mafic dike intrusions (Turkey): Implications for the Neotethyan ocean: Geological Society of America Bulletin, v. 111, p. 1192–1216. doi:10.1130/0016-7606(1999)111<1192:SAPOTO>2.3.CO;2

Dilek, Y., and Whitney, D.L., 1997, Counterclockwise P-T-t trajectory from the metamorphic sole of a Neo-Tethyan ophiolite (Turkey): Tectonophysics, v. 280, p. 295–310. doi:10.1016/S0040-1951(97)00038-3

Edwards, M.A., and Grasemann, B., 2009, Mediterranean snapshots of accelerated slab retreat; subduction instability in stalled continental collision, *in* van Hinsbergen, D.J.J., Edwards, M.A., and Govers, R., eds., Collision and Collapse at the Africa-Arabia-Eurasia subduction zone: Geological Society of London Special Publication, v. 311, p. 155–192.

Erdogan, B., Akay, E., and Ugur, M.S., 1996, Geology of the Yozgat Region and Evolution of the Collisional Cankiri Basin: International Geology Review, v. 38, p. 788–806. doi:10.1080/00206819709465362

Erkan, E., 1976, Isogrades determined in the regional metamorphic area surrounding Kırşehir and their petrological interpretation (in Turkish with English summary): Yerbilimleri, v. 2, p. 23–54.

Espurt, N., Hippolyte, J.-C., Kaymakci, J.C.N., and Sangu, E., 2014, Lithospheric structural control on inversion of the southern margin of the Black Sea Basin, Central Pontides, Turkey: Lithosphere, v. 6, p. 26–34. doi:10.1130/L316.1

Faccenna, C., Jolivet, L., Piromallo, C., and Morelli, A., 2003, Subduction and the depth of convection in the Mediterranean mantle: Journal of Geophysical Research, v. 108, no. B2, p. 2099. doi:10.1029/2001JB001690

Floyd, P.A., Göncüoglu, M.C., Winchester, J.A., and Yalınız, K. M., 2000, Geochemical character and tectonic environment of Neotethyan ophiolitic fragments and metabasites in the Central Anatolian Crystalline Complex, Turkey, *in* Bozkurt, E., Winchester, J.A., and Piper, J.D.A., eds., Tectonics and Magmatism in Turkey and the Surrounding Area. Geological Society, London, Special Publications, v. 173, p. 183–202.

Gaina, C., Torsvik, T.H., van Hinsbergen, D.J.J., Medvedev, S., Werner, S.C., and Labails, C., 2013, The African Plate: A history of oceanic crust accretion and subduction since the Jurassic: Tectonophysics, v. 604, p. 4–25. doi:10.1016/j.tecto.2013.05.037

Gautier, P., Bozkurt, E., Bosse, V., Hallot, E., and Dirik, K., 2008, Coeval extensional shearing and lateral underflow during Late Cretaceous core complex development in the Niğde Massif, Central Anatolia, Turkey: Tectonics, v. 27, p. TC1003. doi:10.1029/2006TC002089

Gautier, P., Bozkurt, E., Hallot, E., and Dirik, K., 2002, Dating the exhumation of a metamorphic dome: Geological evidence for pre-Eocene unroofing of the Nigde Massif (Central Anatolia, Turkey): Geological Magazine, v. 139, p. 559–576. doi:10.1017/S0016756802006751

Gökten, E., and Floyd, P.A., 1987, Geochemistry and tectonic environment of the Şarkışla area volcanic rocks in Central Anatolia, Turkey: Mineralogical Magazine, v. 51, p. 553–559. doi:10.1180/minmag.1987.051.362.09

Göncüoğlu, M.C., 1986, Geochronological data from the southern part (Niğde area) of the Central Anatolian Massif: Bulletin of the Mineral Research and Exploration Institute of Turkey, v. 105–106, p. 83–96.

Göncüoğlu, M.C., Erler, A., Toprak, V., Yalınız, K.M., Küşçü, I., Köksal, S., and Dirik, K., 1993, Orta Anadolu Masifin batı bölümünün jeolojisi, Bolum 3: Orta Kızılırmak Tersiyer Baseninin jeolojik evrimi: Ankara, T.P.A.O. Report, v. 3313.

Göncüoğlu, M.C., Erler, A., Toprak, V., Yalınız, K.M., Olgun, E., and Rojay, B., 1992, Geology of the western part of the Central Anatolian Massif, part 2: Central section: Ankara, Turkish Petroleum Corporation (TPAO) Report, v. 3155, p. 76 (in Turkish).

Göncüoğlu, M.C., Toprak, V., Küşçü, I., Erler, A., and Olgun, E., 1991, Geology of the western part of the Central Anatolian Massif, part 1: Southern section: Ankara, Turkish Petroleum Corporation (TPAO) Report, v. 2909, p. 140 (in Turkish).

Görür, N., Oktay, F.Y., Seymen, I., and Şengör, A.M.C., 1984, Palaeo-tectonic evolution of the Tuzgolu basin complex, Central Turkey: Sedimentary record of a Neo-Tethyan closure, *in* Robertson, A.H.F., and Dixon, J.E., eds., The Geological Evolution of The Eastern Mediterranean. Geological Society, London, Special Publication, v. 17, p. 455–466.

Görür, N., Tüysüz, O., and Şengör, A.M.C., 1998, Tectonic evolution of the Central Anatolian Basins: International Geology Review, v. 40, p. 831–850. doi:10.1080/00206819809465241

Gradstein, F.M., Ogg, J.G., and Smith, A.G., 2004, A geologic time scale 2004: Cambridge, Cambridge University Press.

Gülyüz, E., Kaymakci, N., Meijers, M.J.M., van Hinsbergen, D. J.J., Lefebvre, C.J.C., Vissers, R.L.M., Hendriks, B.W.H., and Peynircioğlu, A.A., 2013, Late Eocene evolution of the Çiçekdağı Basin (central Turkey): Syn-sedimentary compression during microcontinent–continent collision in central Anatolia: Tectonophysics, v. 602, p. 286–299. doi:10.1016/j.tecto.2012.07.003

Gürer, O.F., Sarica-Filoreau, N., Ozburan, M., Sangu, E., and Dogan, B., 2009, Progressive development of the Büyük Menderes Graben based on new data, western Turkey: Geological Magazine, v. 146, p. 652–673.

Hall, R., 2002, Cenozoic geological and plate tectonic evolution of SE Asia and the SW Pacific: Computer-based reconstructions, model and animations: Journal of Asian Earth Sciences, v. 20, p. 353–431. doi:10.1016/S1367-9120(01)00069-4

Hall, R., 2012, Late Jurassic–Cenozoic reconstructions of the Indonesian region and the Indian Ocean: Tectonophysics, v. 570–571, p. 1–41. doi:10.1016/j.tecto.2012.04.021

Hippolyte, J.-C., Muller, C., Kaymakci, N., and Sangu, E., 2010, Dating of the Black Sea Basin: New nannoplankton ages from its inverted margin in the Central Pontides (Turkey), *in* Sosson, M., Kaymakci, N., Stephenson, R.A., Bergerat, F., and Starostenko, V., eds., Sedimentary basin tectonics from the Black Sea and Caucasus to the Arabian Platform. Geological Society, London, Special Publications, v. 340, p. 113–136.

Ilbeyli, N., 2005, Mineralogical–geochemical constraints on intrusives in central Anatolia, Turkey: Tectono-magmatic evolution and characteristics of mantle source: Geological Magazine, v. 142, p. 187–207. doi:10.1017/S0016756805000476

Isik, V., 2009, The ductile shear zone in granitoid of the Central Anatolian Crystalline Complex, Turkey: Implications for the origins of the Tuzgölü basin during the Late Cretaceous extensional deformation: Journal of Asian Earth Sciences, v. 34, p. 507–521. doi:10.1016/j.jseaes.2008.08.005

Isik, V., Lo, C.-H., Göncüoğlu, C., and Demirel, S., 2008, $^{39}Ar/^{40}Ar$ Ages from the Yozgat Batholith: Preliminary Data on the Timing of Late Cretaceous Extension in the Central Anatolian Crystalline Complex, Turkey: The Journal of Geology, v. 116, p. 510–526. doi:10.1086/590922

Isik, V., Uysal, I.T., Caglayan, A., and Seyitoglu, G., 2014, The evolution of intra-plate fault systems in central Turkey: Structural evidence and Ar-Ar and Rb-Sr age constraints for the Savcili Fault Zone: Tectonics, v. 33. doi:10.1002/2014TC003565

Jaffrey, N., and Robertson, A.H.F., 2001, New sedimentological and structural data from the Ecemis Fault Zone, southern Turkey: Implications for its timing and offset and the Cenozoic tectonic escape of Anatolia: Journal of the Geological Society of London, v. 158, p. 1–12.

Jolivet, L., and Brun, J.-P., 2010, Cenozoic geodynamic evolution of the Aegean: International Journal of Earth Sciences, v. 99, p. 109–138. doi:10.1007/s00531-008-0366-4

Jolivet, L., Faccenna, C., and Piromallo, C., 2009, From mantle to crust: Stretching the Mediterranean: Earth and Planetary Science Letters, v. 285, p. 198–209. doi:10.1016/j.epsl.2009.06.017

Kadıoğlu, Y.K., Dilek, Y., and Foland, K.A., 2006, Slab break-off and syncollisional origin of the Late Cretaceous magmatism in the Central Anatolian crystalline complex, Turkey: Geological Society of America Special Paper, v. 409, p. 381–415.

Kadioglu, Y.K., Dilek, Y., Güleç, N., and Foland, K.A., 2003, Tectonomagmatic evolution of bimodal plutons in the Central Anatolian Crystalline Complex, Turkey: The Journal of Geology, v. 111, p. 671–690. doi:10.1086/378484

Kara, H., and Dönmez, H., 1990, 1:100000 scale geological map of Turkey, Kirsehir-G17 sheet: Ankara, General Directorate of Mineral Research and Exploration (MTA), v. 34, p. 1–17 (in Turkish).

Kaymakci, N., Duermeijer, C.E., Langereis, C.G., White, S.H., and Van Dijk, P.M., 2003, Palaeomagnetic evolution of the Cankiri Basin (central Anatolia, Turkey): Implications for oroclinal bending due to indentation: Geological Magazine, v. 140, p. 343–355.

Kaymakcı, N., Özçelik, Y., White, S.H., and van Dijk, P.M., 2009, Tectono-stratigraphy of the Çankiri Basin: Late Cretaceous to early Miocene evolution of the Neotethyan suture zone in Turkey, *in* van Hinsbergen, D.J.J., Edwards, M.A., and Govers, R., eds., Collision and Collapse at the Africa-Arabia-Eurasia subduction zone: Geological Society of London Special Publication, v. 311, p. 67–106.

Kocak, K., and Leake, B.E., 1994, The Petrology of the Ortakoy District and Its Ophiolite at the Western Edge of the Middle Anatolian Massif, Turkey: Journal of African Earth Sciences, v. 18, p. 163–174. doi:10.1016/0899-5362(94)90028-0

Köksal, S., and Göncüoğlu, M.C., 1997, Geology of the Idis Dağı - Avanos area (Nevsehir, Central Anatolia): Mineral Research and Exploration Bulletin, v. 119, p. 41–58.

Köksal, S., Göncüoğlu, M.C., and Floyd, P.A., 2001, Extrusive members of Postcollisonal A-Type Magmatism in Central Anatolia: Karahıdır volcanics, Idis Dagı – Avanos Area, Turkey, International Geology Review, v. 43, p. 683–694.

Köksal, S., Romer, R.L., Göncüoglu, M.C., and Roksay-Köksal, F., 2004, Timing of post-collisional H-type to A-type granitic magmatism: U-Pb Titanite Ages from the Alpine Central Anatolian Granites (Turkey): International Journal of Earth Sciences, v. 93, p. 974–989.

Lee, J.-Y., Marti, K., Severinghaus, J.P., Kawamura, K., Yoo, H.-S., Lee, J.B., and Kim, J.S., 2006, A redetermination of the isotopic abundances of atmospheric Ar: Geochimica Et Cosmochimica Acta, v. 70, p. 4507–4512. doi:10.1016/j.gca.2006.06.1563

Lefebvre, C., 2011 The tectonics of the Central Anatolian Crystalline Complex: A structural, metamorphic and paleomagnetic study: Utrecht Studies in Earth Sciences [PhD Thesis]: Departement Aardwetenschappen, v. 3, 147 p.

Lefebvre, C., Barnhoorn, A., van Hinsbergen, D.J.J., Kaymakci, N., and Vissers, R.L.M., 2012, Reply to Genç and Yürür's comments on: "Late Cretaceous extensional denudation along a marble detachment fault zone in the Kırşehir massif near Kaman, Central Turkey.": Journal of Structural Geology, v. 36, p. 90–93.

Lefebvre, C., Meijers, M.J.M., Kaymakci, N., Peynircioğlu, A. A., Langereis, C.G., and van Hinsbergen, D.J.J., 2013, Reconstructing the geometry of central Anatolia during the late Cretaceous: Large-scale Cenozoic rotations and deformation between the Pontides and Taurides: Earth and Planetary Science Letters, v. 366, p. 83–98. doi:10.1016/j.epsl.2013.01.003

Lefebvre, C.J.C., Barnhoorn, A., van Hinsbergen, D.J.J., Kaymakcı, N., and Vissers, R.L.M., 2011, Late Cretaceous extensional denudation along a marble detachment fault zone in the Kirşehir massif near Kaman, Central Turkey: Journal of Structural Geology, v. 33, p. 1220–1236.

McDougall, I., and Harrison, T.M., 1999, Geochronology and thermochronology by the 40Ar/39Ar method: New York, Oxford University Press.

Meijers, M.J.M., Kaymakci, N., van Hinsbergen, D.J.J., Langereis, C.G., Stephenson, R.A., and Hippolyte, J.-C., 2010, Late Cretaceous to Paleocene oroclinal bending in the Central Pontides (Turkey): Tectonics, v. 29, p. TC4016. doi:10.1029/2009TC002620

Moix, P., Beccaletto, L., Kozur, H.W., Hochard, C., Rosselet, F., and Stampfli, G.M., 2008, A new classification of the Turkish terranes and sutures and its implication for the paleotectonic history of the region: Tectonophysics, v. 451, p. 7–39. doi:10.1016/j.tecto.2007.11.044

Mues-Schumacher, U., and Schumacher, R., 1996, Problems of stratigraphic correlation and new K-Ar data for ignimbrites from Cappadocia, central Turkey: International Geology Review, v. 38, p. 737–746. doi:10.1080/00206819709465357

Okay, A.I., Satir, M., Maluski, H., Siyako, M., Monié, P., Metzger, R., and Akyüz, S., 1996, Paleo- and Neo-Tethyan events in northwestern Turkey: Geologic and geochronologic constraints, *in* Yin, A., and Harrison, T.M., eds., The tectonic evolution of Asia: Cambridge, Cambridge University Press, p. 420–441.

Okay, A.I., Sunal, G., Sherlock, S., Altiner, D., Tüysüz, O., Kylander-Clark, A.R.C., and Aygül, M., 2013, Early Cretaceous sedimentation and orogeny on the active margin of Eurasia: Southern Central Pontides, Turkey: Tectonics, v. 32, p. 1247–1271. doi:10.1002/tect.20077

Okay, A.I., Tansel, I., and Tüysüz, O., 2001, Obduction, subduction and collision as reflected in the Upper Cretaceous–Lower Eocene sedimentary record of western Turkey: Geological Magazine, v. 138, p. 117–142. doi:10.1017/S0016756801005088

Okay, A.I., and Tüysüz, O., 1999, Tethyan sutures of northern Turkey, *in* Durand, B., Jolivet, L., Horvath, F., and Séranne, M., eds., The Mediterranean basins: Tertiary extension within the Alpine Orogen: Special Publication of the Geological Society of London, v. 156, p. 475–515.

Okay, A.I., Tüysüz, O., Satir, M., Özkan-Altiner, S., Altiner, D., Sherlock, S., and Eren, R.H., 2006, Cretaceous and Triassic subduction-accretion, high-pressure–low-temperature metamorphism, and continental growth in the Central Pontides, Turkey: Geological Society of America Bulletin, v. 118, p. 1247–1269.

Oner, Z., and Dilek, Y., 2011, Supradetachment basin evolution during continental extension: The Aegean province of western Anatolia, Turkey: Turkey, Geological Society of America Bulletin, v. 123, p. 2115–2141. doi:10.1130/B30468.1

Oner, Z., and Dilek, Y., 2013, Fault kinematics in supradetachment basin formation, Menderes core complex of western Turkey: Tectonophysics, v. 608, p. 1394–1412. doi:10.1016/j.tecto.2013.06.003

Parlak, O., and Robertson, A.H.F., 2004, The ophiolite-related Mersin Melange, southern Turkey: Its role in the tectonic–sedimentary setting of Tethys in the Eastern Mediterranean region: Geological Magazine, v. 141, p. 257–286. doi:10.1017/S0016756804009094

Plunder, A., Agard, P., Chopin, C., and Okay, A.I., 2013, Geodynamics of the Tavşanlı zone, western Turkey: Insights into subduction/obduction processes: Tectonophysics, v. 608, p. 884–903. doi:10.1016/j.tecto.2013.07.028

Pourteau, A., Candan, O., and Oberhänsli, R., 2010, High-Pressure metasediments in central Turkey: Constraints on the Neotethyan closure history: Tectonics, v. 29, p. TC5004. doi:10.1029/2009TC002650

Pourteau, A., Sudo, M., Candan, O., Lanari, O., Vidal, O., and Oberhansli, R., 2013, Neotethys closure history of Anatolia: Insights from 40Ar- 39Ar geochronology and P-T estimation in high-pressure metasedimentary rocks: Journal of Metamorphic Geology, v. 31, p. 585–606. doi:10.1111/jmg.12034

Renne, P.R., Mundil, R., Balco, G., Min, K., and Ludwig, K.R., 2010, Joint determination of $^{40}K$ decay constants and $^{40}Ar^*/^{40}K$ for the Fish Canyon sanidine standard, and improved accuracy for $^{40}Ar/^{39}Ar$ geochronology: Geochimica et Cosmochimica Acta, v. 74, p. 5349–5367. doi:10.1016/j.gca.2010.06.017

Rice, S.P., Robertson, A.H.F., and Ustaömer, T., 2006, Late Cretaceous-Early Cenozoic tectonic evolution of the Eurasian active margin in the Central and Eastern Pontides, northern Turkey, *in* Robertson, A.H.F., and Mountrakis, D., eds., Tectonic Development of the Eastern Mediterranean Region. Geological Society, London, Special Publications, v. 260, p. 413–445.

Robertson, A., 2004, Development of concepts concerning the genesis and emplacement of Tethyan ophiolites in the Eastern Mediterranean and Oman regions: Earth Science Reviews, v. 66, p. 331–387.

Robertson, A.H.F., Parlak, O., and Ustaömer, T., 2009, Melange genesis and ophiolite emplacement related to subduction of the northern margin of the Tauride-Anatolide continent, central and western Turkey, *in* van Hinsbergen, D.J.J., Edwards, M.A., and Govers, R., eds., Collision and Collapse at the Africa-Arabia-Eurasia subduction zone, Geological Society of London Special Publication, v. 311, p. 9–66.

Sanchez-Gomez, M., Avigad, D., and Heimann, A., 2002, Geochronology of clasts in allochthonous Miocene sedimentary sequences on Mykonos and Paros Islands: Implications for back-arc extension in the Aegean Sea: Journal of the Geological Society of London, v. 159, p. 45–60. doi:10.1144/0016-764901031

Sarıfakıoğlu, E., Dilek, Y., and Winchester, J.A., 2013, Late Cretaceous subduction initiation and Palaeocene–Eocene slab breakoff magmatism in South-Central Anatolia, Turkey: International Geology Review, v. 55, p. 66–87. doi:10.1080/00206814.2012.727566

Seaton, N.C.A., Whitney, D.L., Teyssier, C., Toraman, E., and Heizler, M.T., 2009, Recrystallization of high-pressure marble (Sivrihisar, Turkey): Tectonophysics, v. 479, p. 241–253. doi:10.1016/j.tecto.2009.08.015

Şen, S., and Seyitoğlu, G., 2009, Magnetostratigraphy of early-middle Miocene deposits from E-W trending Alasehir and Büyük Menderes grabens in western Turkey, and its tectonic implications, *in* van Hinsbergen, D.J.J., Edwards, M.A., and Govers, R., eds., Collision and collapse at the Africa-Arabia-Eurasia subduction zone: Geological Society of London Special Publication, v. 311, p. 321–342.

Şengör, A.M.C., Özeren, M.S., Keskin, M., Sakınç, M., Özbakır, A.D., and Kayan, İ., 2008, Eastern Turkish high plateau as a small Turkic-type orogen: Implications for post-collisional crust-forming processes in Turkic-type orogens: Earth-Science Reviews, v. 90, p. 1–48. doi:10.1016/j.earscirev.2008.05.002

Sengör, A.M.C., and Yilmaz, Y., 1981, Tethyan evolution of Turkey: A plate tectonic approach: Tectonophysics, v. 75, p. 181–241. doi:10.1016/0040-1951(81)90275-4

Seymen, I., 1981, Stratigraphy and metamorphism of the Kırşehir Massif around Kaman (Kırşehir - Turkey): Bulletin of the Geological Society of Turkey, v. 24, p. 7–14.

Sherlock, S., Kelley, S., Inger, S., Harris, N., and Okay, A.I., 1999, $^{40}Ar/^{39}Ar$ and Rb-Sr geochronology of high-pressure metamorphism and exhumation history of the Tavsanli Zone,

NW Turkey: Contributions to Mineralogy and Petrology, v. 137, p. 46–58.
Stampfli, G.M., and Borel, G.D., 2002, A plate tectonic model for the Paleozoic and Mesozoic constrained by dynamic plate boundaries and restored synthetic oceanic isochrons: Earth and Planetary Science Letters, v. 196, p. 17–33. doi:10.1016/S0012-821X(01)00588-X
Stampfli, G.M., and Hochard, C., 2009, Plate tectonics of the Alpine realm, *in* Murphy, J.B., Keppie, J.D., and Hynes, A. J., eds., Ancient orogens and modern analogues. Geological Society, London, Special Publications, v. 327, p. 89–111.
Suppe, J., 1983, Geometry and kinematics of fault–bend folding: American Journal of Science, v. 283, p. 684–721. doi:10.2475/ajs.283.7.684
Toprak, V., 1994, Central Kızılırmak Fault Zone: Northern margin of Central Anatolian Volcanics.: Turkish Journal of Earth Sciences, v. 3, p. 29–38.
Torsvik, T.H., Van der Voo, R., Preeden, U., Mac Niocaill, C., Steinberger, B., Doubrovine, P.V., van Hinsbergen, D.J.J., Domeier, M., Gaina, C., Tohver, E., Meert, J.G., McCausland, P.J.A., and Cocks, L.R.M., 2012, Phanerozoic polar wander, palaeogeography and dynamics: Earth-Science Reviews, v. 114, p. 325–368. doi:10.1016/j.earscirev.2012.06.007
Tüysüz, O., Dellaloğlu, A.A., and Terzioğlu, N., 1995, A magmatic belt within the Neo-Tethyan suture zone and its role in the tectonic evolution of northern Turkey: Tectonophysics, v. 243, p. 173–191. doi:10.1016/0040-1951(94)00197-H
van Hinsbergen, D.J.J., Hafkenscheid, E., Spakman, W., Meulenkamp, J.E., and Wortel, M.J.R., 2005, Nappe stacking resulting from subduction of oceanic and continental lithosphere below Greece: Geology, v. 33, p. 325–328. doi:10.1130/G20878.1
van Hinsbergen, D.J.J., Kapp, P., Dupont-Nivet, G., Lippert, P. C., DeCelles, P.G., and Torsvik, T.H., 2011, Restoration of Cenozoic deformation in Asia, and the size of Greater India: Tectonics, v. 30, p. TC5003. doi:10.1029/2011TC002908
van Hinsbergen, D.J.J., Kaymakci, N., Spakman, W., and Torsvik, T.H., 2010, Reconciling the geological history of western Turkey with plate circuits and mantle tomography: Earth and Planetary Science Letters, v. 297, p. 674–686. doi:10.1016/j.epsl.2010.07.024
van Hinsbergen, D.J.J., and Meulenkamp, J.E., 2006, Neogene supra-detachment basin development on Crete (Greece) during exhumation of the South Aegean core complex: Basin Research, v. 18, p. 103–124. doi:10.1111/j.1365-2117.2005.00282.x
van Hinsbergen, D.J.J., and Schmid, S.M., 2012, Map-view restoration of Aegean-west Anatolian accretion and extension since the Eocene: Tectonics, v. 31., p. TC5005. doi:10.1029/2012TC003132
Viereck-Goette, L., Lepetit, P., Gürel, A., Ganskow, G., Çopuroğlu, O., and Abratis, M., 2010, Revised volcanostratigraphy of the Upper Miocene to Lower Pliocene Ürgüp Formation, Central Anatolian volcanic province, Turkey, *in* Groppelli, G., and Viereck-Goette, L., eds., Stratigraphy and Geology of Volcanic Areas: Geological Society of America Special Paper, v. 464, p. 85–112.
Whitney, D.L., and Dilek, Y., 1997, Core complex development in central Anatolia, Turkey: Geology, v. 25, p. 1023–1026. doi:10.1130/0091-7613(1997)025<1023:CCDICA>2.3.CO;2
Whitney, D.L., and Dilek, Y., 2001, Metamorphic and tectonic evolution of the Hirkidag Block, Central Anatolian Crystalline Complex: Turkish Journal of Earth Sciences, v. 10, p. 1–15.
Whitney, D.L., and Hamilton, M.A., 2004, Timing of high-grade metamorphism in central Turkey and the assembly of Anatolia: Journal of the Geological Society of London, v. 161, p. 823–828. doi:10.1144/0016-764903-081
Whitney, D.L., Teyssier, C., Fayon, A.K., Hamilton, M.A., and Heizler, M., 2003, Tectonic controls on metamorphism, partial melting, and intrusion: Timing and duration of regional metamorphism and magmatism in the Niğde Massif, Turkey: Tectonophysics, v. 376, p. 37–60. doi:10.1016/j.tecto.2003.08.009
Whitney, D.L., Teyssier, C., Toraman, E., Seaton, N.C.A., and Fayon, A.K., 2011, Metamorphic and tectonic evolution of a structurally continuous blueschist-to-Barrovian terrane, Sivrihisar Massif, Turkey: Journal of Metamorphic Geology, v. 29, p. 193–212. doi:10.1111/j.1525-1314.2010.00915.x
Yalınız, K.M., and Göncüoğlu, M.C., 1998, General geological characteristics and distribution of the Central Anatolian Ophiolites: Yerbilimleri, v. 20, p. 19–30.
Yalınız, K.M., Güncüoglu, M.C., and Özkan-Altıner, S., 2000, Formation and emplacement ages of the SSZ-type Neotethyan ophiolites in Central Anatolia, Turkey: Palaeotectonic implications: Geological Journal, v. 35, p. 53–68. doi:10.1002/1099-1034(200004/06)35:2<53::AID-GJ837>3.0.CO;2-6
Yürür, M.T., and Genç, Y., 2006, The Savcili thrust fault (Kirsehir region, central Anatolia): A backthrust fault, a suture zone or a secondary fracture in an extensional regime?: Geological Carpathica, v. 57, p. 47–56.
Zachariasse, W.J., van Hinsbergen, D.J.J., and Fortuin, A.R., 2011, Formation and fragmentation of a late Miocene supra-detachment basin in central Crete: Implications for exhumation mechanisms of high-pressure rocks in the Aegean forearc: Basin Research, v. 23, p. 678–701. doi:10.1111/j.1365-2117.2011.00507.x

## Appendix

Analytical data of the $^{40}Ar/^{39}Ar$ dating of andesite from the base of the Ayhan stratigraphy (21-05) (Figure 6). The sample was crushed, sieved, and washed in acetone and distilled water. Plagioclase was separated using standard techniques and fresh inclusion-free mineral grains were handpicked under a binocular microscope.

The transformation $^{39}K(n, p)^{39}Ar$ was performed during irradiation at the IFE Kjeller reactor in Norway, using the Taylor Creek Rhyolite as flux monitor (28.619 ± 0.034 Ma (Renne *et al.* 2010)). Samples were step heated in the $^{40}Ar/^{39}Ar$ laboratory at the Geological Survey of Norway using a Merchantek MIR-10 $CO_2$ laser. The extracted gases were swiped over getters (SAES AP-10) for 2 minutes and then for 9 minutes in a separate part of the extraction line. The peaks were determined by peak hopping (at least eight cycles) on masses $^{41}Ar$ to $^{35}Ar$ on a Balzers electron multiplier on a MAP 215-50 mass spectrometer. Data from unknowns were corrected for blanks (every fourth analysis is a blank) prior to being reduced with the IAAA software package (Interactive Ar-Ar Analysis, written by M. Ganerød, NGU Trondheim, Norway) that implements the equations in McDougall and Harrison (1999) using the decay constants of Renne *et al.* (2010) and the trapped $^{40}Ar/^{36}Ar$ ratio of 298.56 ± 0.31 of (Lee *et al.* 2006). Data reduction in IAAA incorporates corrections for interfering isotopes (based on $K_2SO_4$ and $CaF_2$ salts included in the irradiation package), mass discrimination, error in blanks, and decay of $^{37}Ar$ and $^{39}Ar$.